Research Unit Radiation Cytogenetics
Head: Prof. Dr. rer. nat. Horst Zitzelsberger
Helmholtz Zentrum München

Identification of gene association networks of the cellular radiation response from time-course transcriptomic data

Dissertation
zum Erwerb des Doktorgrades der Naturwissenschaften
an der Medizinischen Fakultät
der Ludwig-Maximilians-Universität zu München

vorgelegt von
Agata Michna

aus
Wodzisław Śląski, Polen

2016

Mit der Genehmigung der Medizinischen Fakultät
der Ludwig-Maximilians-Universität München

Betreuer: Prof. Dr. rer. nat. Horst Zitzelsberger

Zweitgutachterin: Prof. Dr. Anne-Laure Boulesteix

Dekan: Prof. Dr. med. dent. Reinhard Hickel

Tag der mündlichen Prüfung: 03.03.2017

Eidesstattliche Versicherung

Michna, Agata

Name, Vorname

Ich erkläre hiermit an Eides statt,
dass ich die vorliegende Dissertation mit dem Thema

"Identification of gene association networks of the cellular radiation response from time-course transcriptomic data"

selbständig verfasst, mich außer der angegebenen keiner weiteren Hilfsmittel bedient und alle Erkenntnisse, die aus dem Schrifttum ganz oder annähernd übernommen sind, als solche kenntlich gemacht und nach ihrer Herkunft unter Bezeichnung der Fundstelle einzeln nachgewiesen habe.

Ich erkläre des Weiteren, dass die hier vorgelegte Dissertation nicht in gleicher oder in ähnlicher Form bei einer anderen Stelle zur Erlangung eines akademischen Grades eingereicht wurde.

München, 03.03.2017

Ort, Datum

Unterschrift Doktorandin/Doktorand

Contents

Introduction

This thesis explored gene association networks of the radiation response of normal and tumor cells in a therapeutic dose range. These networks were derived from time-course mRNA expression data that required bioinformatic strategies for the analysis of high-dimensional data sets. The gene association networks of sensitive and resistant cells were compared. The novel bioinformatic approach as well as the results from the network reconstructions were published in two peer-reviewed journals and built the basis for this thesis.

Radiation therapy and head and neck cancer

Radiation therapy alone or in combination with surgery and/or drug therapy serves as a fundamental tool for cancer treatments. About 50% of all cancer patients receive curative radiation therapy during their disease [1–3]. However, despite its high effectiveness, radio(chemo)therapy can fail to eradicate all of the clonogenic cancer cells resulting in the relapse of the disease.

Radiotherapy is usually divided in a number of daily fractions to reach the total dose that is needed to treat a particular tumor type which is usually in the range of 50-70 Gy in the case of head and neck squamous cell carcinomas (HNSCC). Importantly, the total dose is applied in a fractionated way (usually 1.8-2 Gy per day) which affects cellular key processes including DNA repair, cell cycle redistribution, repopulation of cells continuing to proliferate and cell reoxygenation [4]. Owing to the fact that the surviving cancer cells are able to regenerate the tumor, repopulation is one of the most common reasons for the failure of conventional fractionated courses of radiation therapy [5–7]. Additionally, there are some evidences that the repopulating tumor cells acquire radioresistance which limits the effectiveness of the radiation therapy [8]. Further, it is well known that tumor subpopulations in hypoxic areas are more radioresistant and thereby are critical to target for increased

therapeutic benefits [9]. Reoxygenation between dose fractions is therefore believed to improve the efficacy of radiotherapy.

Another important factor for therapy success is the intrinsic radiosensitivity of both tumor and normal cells [10]. The intrinsic radiosensitivity of cells describes the phenomenon that cells respond differently to radio(chemo)therapy *a priori*, influencing thereby the overall outcome of the therapy. There is a strong link between intrinsic radiosensitivity and genetic instability of different tumors leading to diverse responses even among tumors of the same histopathology [11]. For this reason, identification of altered signaling pathways involved in the regulation of cell cycle, cell proliferation, DNA response or apoptotic processes might offer the possibility for stratification of poorly responding patients and for personalization of the treatment based on individual features of the tumors. Among different cancers, intrinsic radioresistance has been shown as one of the main reasons of HNSCC recurrence [12].

In Europe, HNSCC develop in approx. 139,000 cases per year with an estimated survival rate of 40% at 5 years after therapy [13]. They originate from the oral cavity, nasopharynx, oropharynx, hypopharynx, or larynx [14]. The most important risk factors include tobacco use, alcohol use, poor oral health and infection with high-risk human papilloma viruses [15–17]. Moreover, HNSCC are very heterogenous in terms of therapy response. Besides, poor prognosis of HNSCC patients is often associated with radioresistance [18]. Therefore, it is of special interest to investigate the molecular mechanisms of HNSCC in order to identify new potential biomarkers of radioresistance and novel therapeutic targets.

Radiation response in normal and tumor tissues

Despite substantial progress in radiotherapy due to the implementation of advanced medical imaging, precise radiation therapy planning, more accurate tumor targeting and development of radiation delivery methods combined with computational technology the radiation response of normal and tumor tissues remains the limiting factor in radiation treatments [19]. Normal tissue responses to ionizing radiation vary greatly between patients. Approximately 5-10% of cancer patients develop severe side effects to external radiotherapy in normal tissue within the treatment

area [20]. The side effects of radiotherapy on normal tissue are classified into acute effects, late effects and secondary cancer induction. Early effects appear during or directly after radiotherapy and manifest erythema and desquamation of the exposed skin and mucosa. Most severe skin and mucosa reactions are seen when radiotherapy is applied in combination with chemotherapy such as cisplatin, methotrexate or actinomycin D. Late effects such as fibrosis, anemia and telangiectasia develop months or years after the end of treatment. Moreover, many organs including heart, spinal cord, brain, kidneys, liver and lung exhibit high radiation sensitivity [21, 22]. In principle, acute or early effects of radiation can be modified by changing the intensity of the treatment. However, up to 70% of the patient and treatment related factors influencing the intraindividual variability of radiation side effects remain unknown [23]. Turesson et al. suggested that the unexplained variability might be associated with individual cellular radiation sensitivity determined by genetic and epigenetic variation [23]. Hence, individual radiation sensitivity became an important therapeutic aspect determining the success of radiotherapy and the ability to modulate patient's radiosensitivity is prerequisite to improve radiotherapy outcome.

For HNSCC it was proposed that fractionated radiation might eradicate radiosensitive cells whereas the radioresistant ones remain largely untouched and therefore, the recurrent tumors mostly consist of radioresistant cells [18, 24]. Although several different mechanisms causing radioresistance have been suggested and extensively studied, the underlying molecular mechanisms remain mostly unknown [25]. To date, three main pathways are known to be associated with radioresistance of HNSCC - EGFR, PI3K/Akt/mTOR and the p53 signaling cascades [18, 26]. However, considering poor overall survival rates for radio(chemo)therapy-treated HNSCC patients it is important to unravel the molecular mechanisms driving radioresistance in order to identify new targets for the modulation of therapeutic response.

Determination of radiation response

The radiation response of normal and HNSCC cells can be measured by determining cell survival or metabolic activity after irradiation. Cell survival is usually determined by the clonogenic (colony formation) assay, which is an in vitro cell survival

assay based on the single cell capability to proliferate and develop a colony. The relationship between applied radiation doses and proportion of survived cells measured as colonies is described by dose-survival curves [27]. Although the colony forming assay was initially introduced for studying the effects of ionizing radiation on cells, nowadays this technique is widely used to examine the effects of different drugs and chemicals that can be considered for clinical applications [28].

The clonogenic assay has been shown to be a reliable method for the detection of radiation sensitive adherent cell lines, but is inconvenient for cells growing in suspension such as the lymphoblastoid cells [29]. In such cases the metabolic activity of mitochondria can be used as an indicator of cell viability. The principle of the so-called WST-1 assay is based on the reduction of the water-soluble tetrazolium salt WST-1 to formazan by cellular dehydrogenases. The concentration of generated dark yellow colored formazan directly correlates with the number of viable cells and therefore, the number of viable cells can be assessed by measuring the absorbance at 420-480 nm [30].

The described approaches reflect either short-term (metabolic activity) or long-term (survival) effects of irradiation, the latter of which is commonly accepted as a "gold standard" to determine cellular radiation response.

Signaling pathways associated with radiation response

DNA is the main cellular target for radiation-induced cancer cell death. Ionizing radiation induces a variety of DNA damages, including sugar and base modifications, oxidized base damage, abasic sites, single strand breaks (SSBs), double strand breaks (DSBs), DNA interstrand cross-links, DNA-proteins cross-links or locally multiply damaged sites [31–34]. The DNA damage repair is crucial to genome integrity and failures in repair have large impact on cell survival after irradiation. Therefore, DNA damage response mechanisms represent very important elements of radiation response.

The first phase of DNA damage response involves the phosphorylation and activation of ATM and ATR kinases, which are responsible for controlling of various downstream signaling pathways [35, 36]. One of these pathways is involved in the regula-

tion of the p53 protein activity. The p53 is one of the most important stress-induced proteins and one of the main cell cycle regulators. Phosphorylation of p53 by ATM or ATR leads to the stabilization of this protein by dissociation from MDM2 and its accumulation in the nucleus. Depending on the phosphorylation site, activation of the p53 protein may lead to cell cycle arrest or to apoptosis [37]. After cell cycle arrest, DSBs are repaired mainly by non-homologous end-joining (NHEJ) and homologous recombination (HR). If the DNA damage is repaired, the cell will continue to divide, otherwise inhibition of the cell proliferative ability may result in cell death or permanent cell cycle arrest, i.e. senescence [38].

Apoptosis and mitotic catastrophe next to autophagy and necrosis are the major and extensively studied radiation-induced forms of cell death [39–41]. However, despite the diverse cell death options, cells developed a stress-induced senescence mechanism to bypass the persistence of radiation-induced DNA damage and avoid possible cancer induction [42]. Regardless of the fact that senescent cells lost the proliferation capability, they remain metabolically active and thereby cannot be considered as dead [43]. Although it is obvious that cancer cell death is a desirable effect of radiation therapy, it is not clear weather senescence has a positive or negative influence on the tumor treatment. On the one hand side, cancer cells that undergo senescence may secret the so-called senescence-associated secretory phenotype factors (SASP), which leads to aggregation of immune cells and activation of an antitumor adaptive immune response. Aggregated immune cells can target transformed or damaged cells and thereby positively contribute to the tumor therapy [44–46]. On the other hand side, the recruitment of immune cells can lead to sustained inflammation and persisting senescence resulting in the induction of cancer or other inflammation-related diseases [47–49]. Continuous senescence can damage local cell environment and thereby stimulate angiogenesis and tumor progression [50–53]. Interestingly, Tsai et al. have reported that the induction of senescence in tumor surrounding normal tissue may increase radiation tolerance or even lead to radioresistance of the tumor [54]. Moreover, recent studies have shown that senescent tumor cells are dormant and might be awaken some time after therapy [42]. Thus, senescence may in some circumstances impose negative effects on the tumor radiotherapy and it might be beneficial to prevent senescence or senescence-associated events in order to avoid acquired radioresistance in tumor cells.

The epidermal growth factor receptor (EGFR) pathway is another pathway affected by ionizing radiation. Ionizing radiation can simulate the process of ligand binding to EGFR and lead to dimerization of the receptor and subsequent activation by autophosphorylation [55]. Activated EGFR initiates the expression of cyclin D1, iNOS and B-MYB promoting cell cycle progression and proliferation [55–57]. In response to ionizing radiation EGFR, particularly in heterodimers with ERBB2, can act anti-apoptotically by transcriptional activation of the anti-apoptotic BCL2L1 gene. Furthermore, EGFR/ERBB2 heterodimers lead to activation of the PI3K/Akt1 pathway, which results in phosphorylation of cell cycle and apoptosis regulatory proteins including IKK and mTOR [58, 59]. Activated by phosphorylation IKK subsequently phosphorylates IkB causing the dissociation of NFκB from IkB. Translocation of the NFκB to the nucleus induces transcription of the anti-apoptotic genes [60]. The activation of mTOR kinase stimulates cell cycle progression, promotes cell survival and inhibits autophagy [61]. Moreover, EGFR may lead to a constant stimulation of the RAS/RAF/MAPK pathway, which for several cancers has been linked with radiation resistance [62–65]. Constantly activated or mutated RAS protein triggers not only the pro-proliferative MAPK pathway but also the pro-survival PI3K/Akt1 pathway [62].

Knowledge of the significance of cellular processes affected by ionizing radiation contributes to the development of strategies, which aim to improve radiation therapy outcome.

Strategies for modulation of radiation response

Strategies to improve radiotherapy outcome intend to increase the tumor response or to decrease the response of normal tissue. Several different approaches including inhibition of DNA repair mechanisms, cell death induction or suppression of survival pathways have been followed in translational radiotherapy research to modulate tumor response to ionizing radiation. Other strategies employ drugs that act as radioprotectors by preventing normal tissues from radiation damage without affecting tumor radiosensitivity.

Prophylactic, mitigators and therapeutic agents are the three types of normal tissue radiation responses modifiers [66]. Prophylactic or protector agents are given before the radiotherapy and include free radical scavengers, inhibitors of p53 and antioxidant mediators that prevent from initialization of radiochemical events, early apoptotic cell death and inflammation. Mitigators given at the time of right after ionizing radiation exposure include antioxidants, growth factors and methods using stem cells or progenitor cells that trigger regeneration, proliferation and survival of healthy normal tissue.

Numerous chemotherapeutic anti-cancer drugs have been used to sensitize cells to radiation including 5-fluorouracil, actinomycin D, cisplatin, gemcitabine, fludarabine, paclitaxel, doxorubicin, hydroxyurea, mitomycin C, topotecan, or vinorelbine. The radiosensitization mechanism differs between the chemotherapeutic agents. Cisplatin, carboplatin, oxaliplatin and other platinum-containing chemotherapeutics show the ability to crosslink with the purine bases on the DNA, suppressing the DNA repair mechanisms, causing DNA damage, and subsequently leading to apoptotic cancer cells death [67]. The radiosensitizing properties of topotecan can be explained by the inhibition of DNA repair mechanisms namely inhibition of the topoisomerase [68]. The proposed mechanisms of doxorubicin action are twofold and include the intercalation to DNA followed by disruption of DNA repair and the generation of reactive oxygen species resulting in DNA, proteins and cellular membrane damage [69]. Mitomycin C is more effective in sensitizing hypoxic cells [70]. Hydroxyurea leads to the inhibition of DNA synthesis and subsequent cell death in S-phase of the cell cycle. Additionally, it prevents entry to the G1-phase synchronizing the survival fraction of cells [71], whereas paclitaxel block cells in the G2/M-phase disabling normal mitosis [72].

In HNSCC the EGFR is one of the key deregulated signaling pathways. Overexpression of EGFR in HNSCC is a strong and unfavorable prognostic factor [26, 73, 74]. The importance of the EGFR and its downstream PI3K/Akt/mTOR, NFκB and MAPK survival pathways led to the development of small-molecule inhibitors and blocking antibodies. Cetuximab to date was the most commonly used EGFR-specific antibody, which substantially increased local-regional control in the first phases of radiochemotherapy treatments [75, 76]. However, recent studies have identified sig-

naling pathways activated by mutated KRAS, BRAF and NRAS genes that bypas EGFR and mediate cetuximab radioresistance. Therefore, the use of cetuximab is currently limited to patients who do not harbor KRAS mutations [77]. Accordingly, inhibition of EGFR remains a challenge as complex networks are involved in the EGFR signal propagation [78, 79]. The presence of strong feedback loops frequently lower the effect of radiation therapy and often only specific combinations of inhibitors are effective [80–86]. Therefore, one of the major challenges in targeted cancer therapy is the prediction of effective combinatorial treatments [87]. Molecular systems biology and mathematical modeling of signaling networks can facilitate understanding of the role and functions of these networks and help finding the most suitable treatment.

Implications of microarrays in clinical oncology

Analysis of genomic and transcriptomic data has contributed to a large number of biological and clinical research studies. Microarray technology has been effectively used for genome-wide expression profiling of various development processes, treatments and diseases. Since its development in the middle of the 1990s, microarray technology has been extensively used to understand and improve the knowledge of complex experimental, scientific and medical problems. Traditional research has mainly focused on functions of single genes involved in the development of a disease. However, results based on investigations of individual genes can be misleading due to the fact that single-gene inquiry ignores the high complexity of the gene regulatory network in which the gene of interest might be involved. One great advantage of microarray technology is that it enables the investigation of the entire genome simultaneously in a single experiment. This allows a better comprehension of the gene regulations and signaling networks that might be concealed in single-gene based studies [88].

Analysis of expression patterns across hundreds of clinical samples has been shown to facilitate disease diagnosis, risk stratification and determination of therapeutic regimens for specific groups of patients [89]. Carcinogenesis and cancer progression are certainly one of the predominant focuses of microarray-based studies. Microarrays have been widely used to analyze different types of tumor, including breast,

lung, leukemia, ovary, prostate, colorectal, head and neck, lymphoma and melanoma [90–105]. Owing to the fact that gene expression plays a crucial role in determining the clinical behavior of tumors, identification of expression patterns and underlying mechanisms are the key aspects, essential for tumor therapy improvements. Microarray technology offers the opportunity to extensively investigate tissue and genotype specific transcriptional changes. Thus, it became a tool that enables prediction of clinical outcome and helps to explore deregulated molecular mechanisms of complex diseases.

Microarray technology

Microarray is a technology in which thousands of short, synthetic, single-stranded DNA sequences are spotted on a solid surface, usually on a glass slide. Each printed spot is typically not larger than 200 microns in diameter and contains multiple identical and unique DNA oligonucleotides. Single microarray comprises of thousands of different spotted samples (known as probes) representing single genes. During the hybridization step, fluorescently labeled RNA or DNA samples of interest are matched with annotated microarray probes based on nucleic acid sequence homology. The amount of RNA or DNA bound to each spot indicates the expression levels [106].

Two types of microarrays were used in the presented thesis, the two-channel comparative genomic hybridization and the single-channel gene expression microarrays. The schematic workflow for the sample preparation and microarray processing for those two microarray types is presented and described in Figure 1.

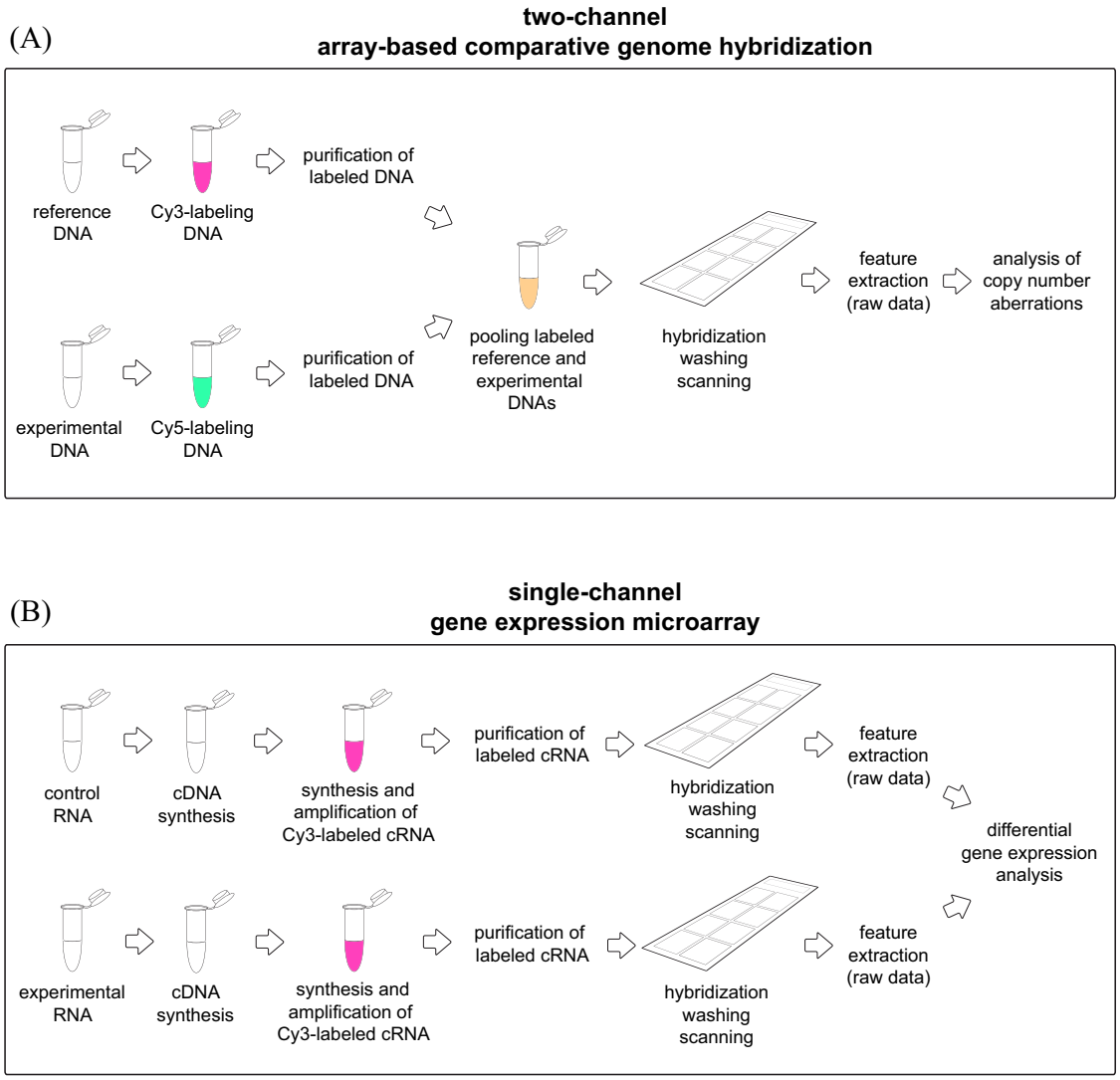

Figure 1. Schematic workflow for sample preparation and microarray processing. The upper panel (A) illustrates the two-channel array-based comparative genomic hybridization (aCGH) technology and the lower panel (B) shows the single-channel gene expression (GE) microarray technology. For the aCGH the reference and the experimental DNA samples are labeled with two different fluorescent dyes (Cy3 and Cy5) and pooled before being hybridized on the same array. For the GE microarrays each sample is labeled with the same fluorescent dye (Cy3), but independently hybridized on different arrays.

Studying and modeling dynamics in biological processes

Gene expression can be studied from a static or temporal point of view. Static experiments allow measuring transcriptional responses at one pre-defined time point capturing only a snapshot of the gene expression. However, most of the biological processes are dynamic and the expression of a gene can vary greatly with time [107]. Therefore, hypotheses build on single-time-point experiments may be misleading and not realistic for understanding complex biological processes. Different sets of genes have different kinetics of response to different stimuli. Consequently, the complete response can be only modeled when the process is followed at numerous time points.

In general, time-course studies can be classified into three experimental types, depending on the design of the study and study interests [108]. The first type has one experimental condition and a corresponding development phase. Accordingly, all time points are examined in contrast to the first time point, which is considered as a control. However, this experimental study type does not provide a proper control over the entire time-course which is a major disadvantage of this approach. The second experimental type categorizes studies with a factorial time-course design that consider multiple treatment conditions simultaneously. This design includes at least two treatment conditions that for a given time point have different temporal expression patterns. Here, the time-course data from one treatment group is compared to the time-course data of the other treatment group(s). Thus, this approach ensures better control of the experiment on the grounds that compared samples are probed over time in parallel. Additionally, the comparison of the gene expression patterns between the treatment groups can be performed independently at any time point. However, in light of the fact that this approach requires more samples, the performance is considerably more expensive. The third type of time-course studies includes periodic and cyclic experiments (e.g. cell cycle), where the main research interests are focused on repeated expression patterns.

Analyses of the time-course experiments in principle follow the same workflow as static experiments (Figure 2). However, comparing to the static data, the analysis of time-course data introduces a number of new challenges. First, the computational complexity of data analysis increases with the increase in the number of feature points. Second, hidden correlation caused by co-expression of genes makes the data

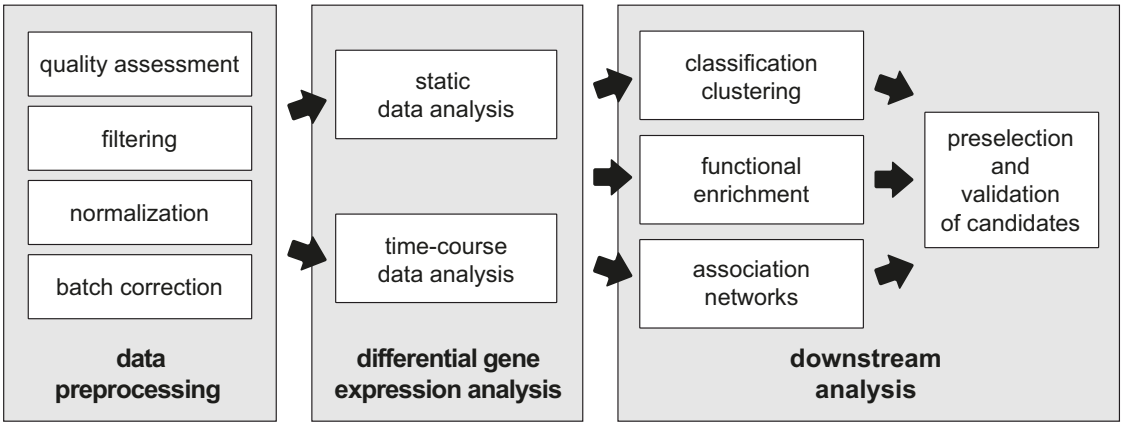

Figure 2. Overview on different modalities of transcriptomic data analysis. Time-course experiments follow the same workflow as static experiments and can be divided into three parts: 1) data preprocessing by data quality assessment, filtering, normalization and batch correction; 2) differential gene expression analyses; and 3) downstream analyses including classification and clustering methods, functional enrichment analyses, gene association networks reconstructions and validation of candidate genes.

linearly dependent [109]. Finally, one has to be aware of additional correlations existing between neighboring time points explicitly disclosed and illustrated in published gene expression profiles [110].

Despite all the existing difficulties of temporal gene expression data analysis, such data can be used to systematically characterize functions of particular genes and to infer their interactions with other genes. This knowledge holds the promise of explaining the relevant mechanisms of different biological processes and may facilitate the molecular target identification of novel pharmaceutical drugs [111]. Therefore, the analyses of the cellular radiation response presented in both of my publications were based on the second experimental type time-course study design to be able to explore the gene expression dynamics.

Gene association networks

Multidimensional datasets from gene expression microarray experiments are nowadays extensively used to uncover unknown relationships between genes. Elucidating networks, which delineate signaling pathways and regulatory mechanisms coordinating multiple molecular processes is one of the most important aims of systems biology.

The process of gene association network reconstruction known also as "reverse engineering" aims to model the complex cellular regulatory interactions and propose a realistic illustration of gene regulation. Several different methods have been suggested and used to reconstruct gene association networks (GANs) including graph theory, Boolean and Bayesian networks, ordinary differential equations, machine learning or correlation approaches [112, 113]. Moreover, the revealed network topologies provide the information how the organization of genes in the network influences their functions and dynamic responses [114].

In both publications of this thesis the GAN reconstructions of temporally differentially expressed genes following radiation were performed using the regularized dynamic partial correlation method [115]. The topological properties of obtained networks were addressed with three different centrality measures (degree, closeness and shortest path betweenness) in order to identify nodes with strategic positions for controlling the network.

The degree centrality is the measure of gene communication activity and defines the number of other genes (nodes) that are directly connected to the gene of interest. Closeness centrality is described as the inverse of the sum of distances of a single gene to other genes. A gene in the closest position to all others can most efficiently attain and pass signals in the network. Betweenness centrality of a node is defined as the ratio between the number of shortest paths passing through the given gene and the number of shortest paths between any pair of genes. This shows the potential of a gene for controlling the signal transduction within the network [116–118].

Publication I of this thesis provided the methodological basis to explore the radiation response in normal and HNSCC cells (publication II) by focussing on the following aims.

Aims and objectives

The overall aim of my thesis was to develop a statistical approach that allows studying the molecular mechanisms of temporal gene expression responses from time-course global transcriptomic data. To reach this aim a number of specific aims had to be addressed. The first one comprised the design and implementation of an algorithm based on natural cubic spline regression models for the detection of temporally differentially expressed genes between different treatment groups. Further, the identified genes were used as prior selection for subsequent gene association network reconstruction by employing regularized dynamic partial correlation method. With this method, I aimed to determine dependencies between the differentially expressed genes based on their expression behavior.

The major challenge in the analysis of high-dimensional expression data sets is the assessment of which single genes or entire cellular processes are the most relevant ones in the case study. Therefore, subsequent topological analysis of the reconstructed networks by a hybrid centrality measure aimed to define a subset of nodes that are likely to play an important role in controlling the signal transduction within the networks. The identified so-called hub genes were then subjected to pathway enrichment analysis, which allowed determining the possibly relevant cellular mechanisms involved in the current study. The objective of the presented approach was the reduction of the number of candidate biological processes being used as hypotheses for further validation in follow-up experiments.

Another important aim of my thesis was the application of the proposed algorithm on two data sets of normal and tumor cell culture models with different cellular radiation sensitivity. With the obtained results I aimed to provide insights into the mechanisms of acute radiation response of the hypersensitive non-tumor lymphoblastoid cells in comparison to the lymphoblastoid cells with normal radiation sensitivity. Moreover, with the presented approach I attempted to indicate the molecular differences of radiation responses in the radioresistant HNSCC derived CAL-33 cell lines with altered acquired radiation sensitivity.

The precise mechanisms behind the acute radiation response of normal cells and tumor radioresistance are still largely unknown [25, 119, 120]. Therefore, within

this thesis I aimed to find clinically relevant molecular targets that could serve as modulators of radiation sensitivity in order to improve tumor radiotherapy outcome.

Summary

The major therapeutic aim of radiotherapy is the maximization of tumor tissue eradication whilst preserving the surrounding normal tissue. Thus, the underlying cellular radiation response is the most important determinant of the radiotherapy success in tumor treatment and the ability to modulate radiosensitivity is a prerequisite to improve the therapy outcome. Despite numerous experimental and clinical studies on radiation sensitivity in different cell types, the molecular mechanisms of acute radiation response and tumor radioresistance still remain unclear. So far, the major limitation of many previous studies was the consideration of single molecular levels or the usage of only static data in order to unravel molecular mechanisms of radiation response. However, biological processes are dynamic and therefore, the integration of time-course data is essential.

In my thesis I have proposed and developed a statistical approach that allows studying molecular mechanisms of temporal gene expression responses from a time-course global transcriptomic data. The approach comprised three major steps: 1) the identification of differentially expressed genes from time-course expression data by employing natural cubic spline regression models (NCSRM); 2) the use of regularized dynamic partial correlation to infer gene associations networks (GANs) from differentially expressed genes; and 3) the topological identification and functional characterization of the key nodes in the reconstructed networks. Subsequently, the proposed approach was applied on a time-resolved transcriptome data set of radiation-perturbed cell culture models of: 1) monoclonal lymphoblastoid cell lines (LCLs) with normal and increased radiation sensitivity and 2) HNSCC-derived CAL-33 cell lines with different acquired radiation resistance.

Two lymphoblastoid cell lines with increased and normal radiation sensitivity that served as cell culture models of normal cells, were irradiated with γ-irradiation at two different doses (1 Gy and 10 Gy). The changes in mRNA expression levels were studied over time within 24 hours following radiation. Gene association networks were

determined and the obtained results underlined the impact of senescence-associated pathways in acute radiation response of normal cells.

Several HNSCC-derived CAL-33 cell lines, with altered acquired radiation sensitivity after fractionated radiation treatment, were used as models of radioresistant tumor cells. The cell lines showing different radiation phenotypes were investigated at the genomic and transcriptomic levels in order to identify mechanisms responsible for distinct radiation responses. Furthermore, the cells were irradiated with X-rays at a dose of 8 Gy (dose showing the most pronounced phenotypical changes) and the mRNA gene expressions were investigated within 4 days following radiation in a time-course study design. Following network reconstruction a key finding was the important role of senescence-associated secretory phenotype (SASP) and GPCR ligand binding pathways for the resistant phenotype response.

The results of the studies obtained using the novel approach generate hypotheses about genes and signaling networks that may play a crucial role in the investigated processes. Thus, the proposed method is able to contribute to a better understanding of the underlying molecular mechanisms and targets that are involved in the radiation response of human cells and by this providing a starting point for an improvement of radiotherapy outcome.

Zusammenfassung

Strahlentherapie verfolgt als wichtigstes therapeutisches Ziel die maximale Eliminierung von Tumorgewebe bei gleichzeitiger Schonung des umgebenden Normalgewebes. Aus diesem Grund ist die zugrunde liegende zelluläre Strahlenantwort der bestimmende Faktor für den Erfolg der Strahlentherapie und demnach die Möglichkeit zur Modulation der Strahlenempfindlichkeit die Voraussetzung für eine Verbesserung des Therapieverlaufs. Trotz zahlreicher experimenteller und klinischer Studien zur Strahlenempfindlichkeit in verschiedenen Zelltypen sind die molekularen Mechanismen der akuten Strahlenantwort und Strahlenresistenz von Tumoren bislang nur unzureichend verstanden. Viele bisherige Studien waren dadurch limitiert, dass nur einzelne molekularen Ebenen betrachtet wurden oder ausschließlich statische Daten verwendet wurden. Alle biologischen Prozesse sind allerdings dynamisch und somit ist für die vollständige Charakterisierung der molekularen Mechanismen der Strahlenantwort die Integration von zeitabhängigen Daten unabdingbar.

Im Rahmen dieser Dissertation habe ich einen statistischen Forschungsansatz entwickelt, der - ausgehend von zeitabhängigen globalen Transkriptionsdaten - die zeitaufgelöste Analyse von Genexpressionsdaten ermöglicht. Dieser Forschungsansatz berücksichtigt drei wesentliche Schritte: 1) die Identifizierung von differentiell exprimierten Genen ausgehend von zeitaufgelösten Genexpressionsdaten durch Anwendung sogenannter Regressionsmodelle mit natürlichen kubischen Spline-Basisfunktionen; 2) die Anwendung von regularisierter dynamischer partieller Korrelation für die Ableitung von Gen-Assoziations-Netzwerken ausgehend von differentiell exprimierten Genen und 3) die topologische Identifizierung und funktionelle Charakterisierung von zentralen Knoten in den rekonstruierten Netzwerken. Die entwickelte Methode wurde auf zeitaufgelöste Transkriptionsdaten strahlenbehandelter Zellkulturmodellen angewandt: 1) von monoklonalen lymphoblastoiden Zellinien (LCLs) mit jeweils normaler und erhöhter Strahlenempfindlichkeit und 2) von HNSCC CAL-33 Zelllinien mit einer unterschiedlichen erworbenen Strahlenresistenz.

Einerseits wurden zwei lymphoblastoide Zelllinien mit normaler und erhöhter Strahlenempfindlichkeit, welche als Zelllinien Modell für Normalzellen verwendet wurden, mit zwei verschiedenen Dosen (1 Gy und 10 Gy γ-Strahlung) bestrahlt. Die Änderungen in der Genexpression wurden über einen Zeitraum von 24 Stunden nach Bestrahlung untersucht. Die Ergebnisse der Netzwerkrekonstruktion zeigten die Bedeutung von Seneszenz-assoziierten Signalwegen bei der akuten Strahlenantwort von Normalzellen.

Andererseits wurden HNSCC CAL-33 Zelllinien mit unterschiedlicher erworbener Strahlenempfindlichkeit als Modelle für strahlenresistente Tumorzellen verwendet. Die Zelllinien, welche unterschiedliche Phänotypen nach Bestrahlung zeigten, wurden auf genomischer und transkiptomischer Ebene untersucht, um Mechanismen der Strahlenantwort zu identifizieren. Dabei wurden die Zellen mit 8 Gy Röntgenstrahlung (die Dosis mit den stärksten phänotypischen Unterschieden) bestrahlt und die Genexpressionen zeitabhängig während der folgenden vier Tage nach Bestrahlung bestimmt. Nach Netzwerkrekonstruktion trat die Bedeutung des Seneszenz -assoziierten sekretorischen Phänotyps (SASP) und des GPCR ligand binding Signalwegs für die Ausprägung einer resistenten Strahlenantwort zu Tage.

Die Ergebnisse der durchgeführten Studien unter Verwendung des neuartigen statistischen Ansatzes haben zu Hypothesen über Gene und Signalnetzwerke geführt, die eine entscheidende Rolle bei der Strahlenantwort von Tumor- und Normalzellen spielen könnten. Somit kann die neu entwickelte statistische Methode dazu beitragen, die der Strahlenantwort von menschlichen Zellen zugrunde liegenden molekularen Mechanismen aufzuklären, die ihrerseits Ansatzpunkte für eine Verbesserung des klinischen Verlaufs nach Strahlentherapie darstellen.

Publications

PLOS ONE journal scope and standing

PLOS ONE is a broad scope multidisciplinary open access journal that publishes original research from all disciplines within science and medicine. It also considers contributions describing new and improved methods, software, databases, and other methodological tools with preference for interdisciplinary studies. PLOS ONE in 2015 has achieved an impact factor of 3.057 and took rank 42 out of 207 journals in the category of biochemistry, genetics and molecular biology.

Radiation Oncology journal scope and standing

Radiation Oncology covers all research that has influence on cancer using radiation therapy. Focus is given on experimental work in radiobiology, radiation physics and technology, planning of radiation treatments, multimodal treatment approaches, and clinical oncology. Journal aims to provide an open access forum for collaboration and knowledge exchange in the management and treatment of cancer patients. For 2015, Radiation Oncology has achieved an impact factor of 2.466 and took rank 40 out of 258 journals in the category of radiology, nuclear medicine and imaging.

Supporting information for both publications can be found at http://journals.plos.org/plosone/ and https://ro-journal.biomedcentral.com/.

PLOS ONE

RESEARCH ARTICLE

Natural Cubic Spline Regression Modeling Followed by Dynamic Network Reconstruction for the Identification of Radiation-Sensitivity Gene Association Networks from Time-Course Transcriptome Data

Agata Michna[1], Herbert Braselmann[1,2], Martin Selmansberger[1], Anne Dietz[3], Julia Hess[1,2], Maria Gomolka[3], Sabine Hornhardt[3], Nils Blüthgen[4], Horst Zitzelsberger[1,2], Kristian Unger[1,2]*

1 Research Unit Radiation Cytogenetics, Helmholtz Zentrum München, German Research Center for Environmental Health GmbH, Neuherberg, Germany, **2** Clinical Cooperation Group "Personalized Radiotherapy in Head and Neck Cancer", Helmholtz Zentrum München, Neuherberg, Germany, **3** Department of Radiation Protection and Health, Federal Office for Radiation Protection, Neuherberg, Germany, **4** Institute of Pathology, Charité—Universitätsmedizin Berlin, Berlin, Germany

* unger@helmholtz-muenchen.de

Citation: Michna A, Braselmann H, Selmansberger M, Dietz A, Hess J, Gomolka M, et al. (2016) Natural Cubic Spline Regression Modeling Followed by Dynamic Network Reconstruction for the Identification of Radiation-Sensitivity Gene Association Networks from Time-Course Transcriptome Data. PLoS ONE 11(8): e0160791. doi:10.1371/journal.pone.0160791

Editor: Geraldo A Passos, University of São Paulo, BRAZIL

Received: April 26, 2016

Accepted: June 14, 2016

Published: August 9, 2016

Data Availability Statement: Expression microarray data files are available from the ArrayExpress database (accession number E-MTAB-4829).

Funding: ZiSS project, 02NUK024B, https://www.bmbf.de/en/index.html, Federal Ministry of Education and Research, KU JH HZ. The funders had no role in study design, data collection and analysis, decision to publish, or preparation of the manuscript.

Competing Interests: The authors have declared that no competing interests exist.

Abstract

Gene expression time-course experiments allow to study the dynamics of transcriptomic changes in cells exposed to different stimuli. However, most approaches for the reconstruction of gene association networks (GANs) do not propose prior-selection approaches tailored to time-course transcriptome data. Here, we present a workflow for the identification of GANs from time-course data using prior selection of genes differentially expressed over time identified by natural cubic spline regression modeling (NCSRM). The workflow comprises three major steps: 1) the identification of differentially expressed genes from time-course expression data by employing NCSRM, 2) the use of regularized dynamic partial correlation as implemented in GeneNet to infer GANs from differentially expressed genes and 3) the identification and functional characterization of the key nodes in the reconstructed networks. The approach was applied on a time-resolved transcriptome data set of radiation-perturbed cell culture models of non-tumor cells with normal and increased radiation sensitivity. NCSRM detected significantly more genes than another commonly used method for time-course transcriptome analysis (BETR). While most genes detected with BETR were also detected with NCSRM the false-detection rate of NCSRM was low (3%). The GANs reconstructed from genes detected with NCSRM showed a better overlap with the interactome network Reactome compared to GANs derived from BETR detected genes. After exposure to 1 Gy the normal sensitive cells showed only sparse response compared to cells with increased sensitivity, which exhibited a strong response mainly of genes related to the senescence pathway. After exposure to 10 Gy the response of the normal sensitive

cells was mainly associated with senescence and that of cells with increased sensitivity with apoptosis. We discuss these results in a clinical context and underline the impact of senescence-associated pathways in acute radiation response of normal cells. The workflow of this novel approach is implemented in the open-source Bioconductor R-package splineTimeR.

Introduction

In general terms, the expression of genes can be studied from a static or temporal point of view. Static microarray experiments allow measuring gene expression responses only at one single time point. Therefore, data obtained from those experiments can be considered as more or less randomly taken snapshots of the molecular phenotype of a cell. However, biological processes are dynamic and thus, the expression of a gene is a function of time [1]. To be able to understand and model the dynamic behavior and association of genes, it is important to study gene expression patterns over time.

However, compared to static microarray data, the analysis of time-course data introduces a number of new challenges. First, the experimental costs for the generation of data as well as the computational cost increases with the increase in the number of introduced time points. Second, hidden correlation caused by co-expression of genes makes the data linearly dependent [2]. Finally, one has to be aware of additional correlations existing between neighboring time points clearly revealed in published gene expression profiles [3].

Several different algorithms have been suggested to analyze gene time-course microarray data with regard to differential expression in two or more biological groups (e.g. exposed to radiation vs. non-exposed) [4–7]. Nevertheless solitary identification of differentially expressed genes does not help to determine the molecular mechanisms in the investigated biological groups. Therefore, it is not only important to know differentially expressed genes per se, but also how those genes interact and regulate each other in order to determine specifically deregulated molecular networks.

Currently, many different algorithms including cluster analysis [8–13] and supervised classification [14–16] are used to identify relationships between genes. However, both of these methods suffer from serious limitations. First, the timing information of the measurements is not incorporated and, therefore, the intrinsic temporal structure of the time-course data is neglected. Second, the available standard clustering and classification methods are not designed to measure statistical significance of the results based on a statistical hypothesis test. By nature of these methods, clusters or classes of genes with similar expression patterns will always be identified but they do not provide a measure of how reliable this information is. For this reason, we preferred usage of a dynamic network modeling approach that allows delineation of relationships between genes along with providing statistical significance for these relationships.

The aim of the present study was to identify and compare signaling pathways involved in the radiation responses of normal cells differing in their radiation sensitivity that could be used to modulate cell sensitivity to ionizing radiation. For this, we propose an approach that combines the detection of genes differentially expressed over time based on statistics determined by natural cubic spline regression (NCSRM) [17] followed by dynamic gene association network (GAN) reconstruction based on a regularized dynamic partial correlation as implemented in the GeneNet R-package [18].

Most exploratory gene expression studies focus only on the identification of differentially expressed genes by treating them as independent events and do not seek to study the interplay of identified genes. This makes it difficult to tell which genes are part of the interaction network

causal of the studied phenotype and which are the most "important" with regard to the context of the investigation. The herein present approach combines the identification of differentially expressed genes and reconstruction of possible associations between them. Further analysis of identified GANs then allows hypothesizing which genes may play a crucial role in the investigated processes. This should markedly increase the likelihood to find meaningful results from an initial observation and help to understand the underlying molecular mechanisms. We applied our workflow on time-course transcriptome data of two normal and well-characterized lymphoblastoid cell lines with normal (20037–200) and increased radiation sensitivity (4060–200), in order to identify molecular mechanisms and potential key players responsible for different radiation responses [19, 20]. Our exploratory approach provides novel and informative insights in the biology of radiation sensitivity of non-tumor cells after exposure to ionizing radiation with regard to the identified signaling pathways and their key drivers. Moreover, we could demonstrate that spline regression in differential gene expression analysis for the purpose of prior selection in gene-association network reconstruction outperforms another commonly used existing approach for time-course gene expression analysis.

Results

The schematic workflow of the presented novel approach for time-course gene expression data analysis is presented in Fig 1.

Identification of ionizing radiation-responsive genes using NCSRM method

A fraction of the probes was removed due to low expression levels, with not detectable signal intensities as described in [21]. Table 1 shows the number of probes remained after quality filtering from the total number of 25220 unique probes representing HGNC annotated genes. Differential analysis was performed relative to the corresponding sham irradiated cells as a reference. In general, more genes were detected as differentially expressed in the cells with increased radiation sensitivity compared to cells with normal radiation sensitivity after each dose of gamma irradiation (Table 1). The most prominent difference was observed when comparing the responses after 1 Gy irradiation. In the cells with increased radiation sensitivity 2335 genes showed differential expression compared to only seven genes in cells with normal radiation sensitivity. We observed the same trend after irradiation with 10 Gy where the cells with increased sensitivity showed 6019 and the normal sensitive cells 3892 differentially expressed genes.

Pathway enrichment analysis of NCSRM identified genes

Pathway enrichment analysis was performed on differentially expressed genes to identify over-represented biological pathways. The analysis on genes identified with NCSRM revealed 634 and 964 significantly enriched pathways for the cells with increased radiation sensitivity after 1 Gy and 10 Gy irradiation dose, respectively and 758 pathways for the normal sensitive cell line after 10 Gy irradiation. For the seven differentially expressed genes (i.e. FDXR, BBC3, VWCE, PHLDA3, SCARF2, HIST1H4C, PCNA) of the cell line with normal radiation sensitivity after 1 Gy dose of irradiation we did not find any significantly enriched pathways. A summary of the pathway enrichment results can be found in S2 Table.

Gene association network reconstruction

None of the edge probabilities calculated for the seven differentially expressed genes in the cell line with normal radiation sensitivity after 1 Gy irradiation exceeded the considered

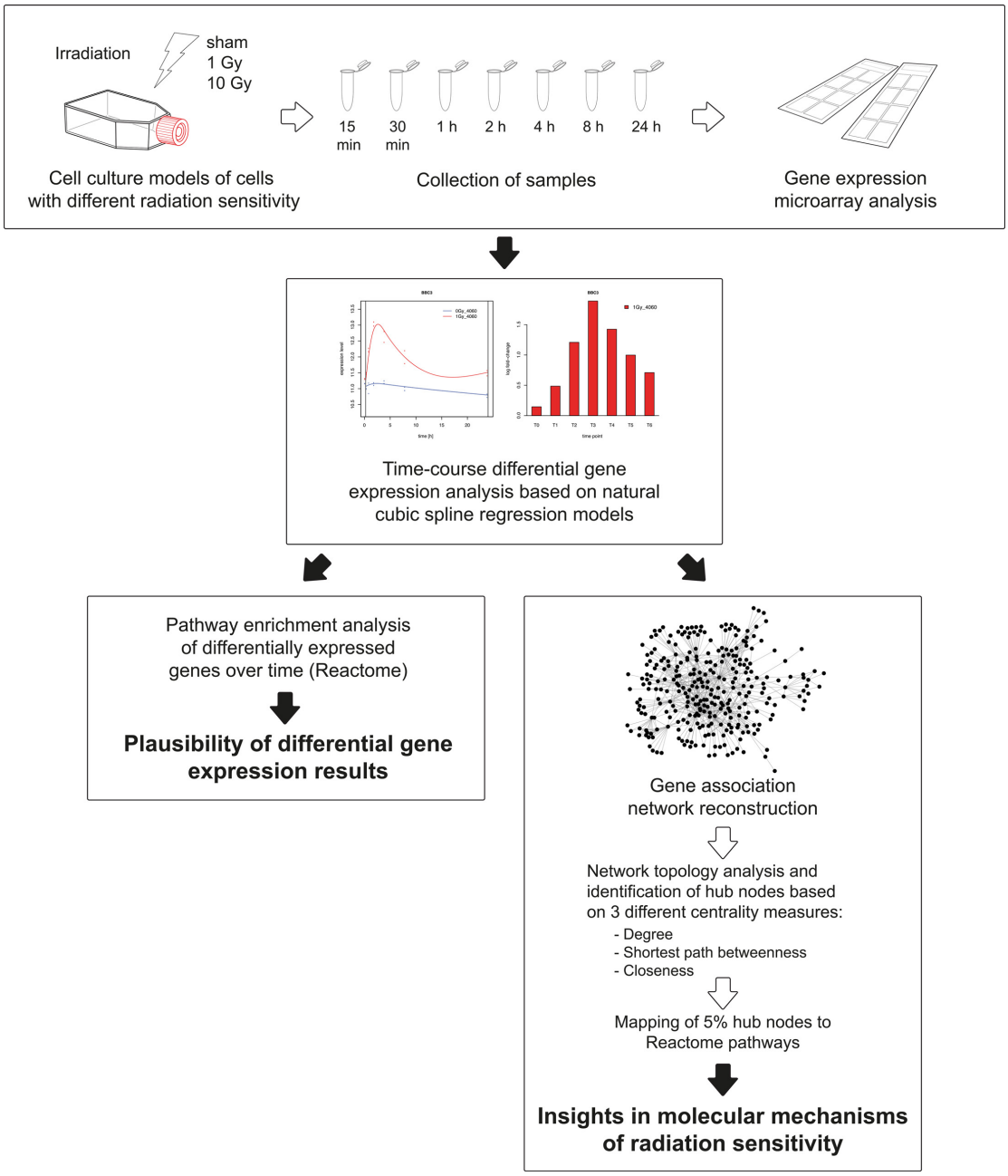
Irradiation
sham
1 Gy
10 Gy
15 min
30 min
1 h
2 h
4 h
8 h
24 h
Cell culture models of cells with different radiation sensitivity
Collection of samples
Gene expression microarray analysis
Time-course differential gene expression analysis based on natural cubic spline regression models
Pathway enrichment analysis of differentially expressed genes over time (Reactome)
Plausibility of differential gene expression results
Gene association network reconstruction
Network topology analysis and identification of hub nodes based on 3 different centrality measures:
- Degree
- Shortest path betweenness
- Closeness
Mapping of 5% hub nodes to Reactome pathways
Insights in molecular mechanisms of radiation sensitivity

Fig 1. Schematic workflow of the analysis of gene expression time-course data. Samples were collected 0.25, 0.5, 1, 2, 4, 8 and 24 hours after sham or actual irradiation. Transcriptional profiling was performed using Agilent gene expression microarrays and comprises three major steps: the identification of differentially expressed genes from time-course expression data by employing a natural cubic spline regression model; the use of regularized dynamic partial correlation method to infer gene associations networks from differentially expressed genes and the topological identification and functional characterization of the key nodes in the reconstructed networks.

doi:10.1371/journal.pone.0160791.g001

significance threshold and hence no network was obtained. For the remaining conditions we were able to obtain association networks as presented in Table 2. Obtained networks are provided as igraph R-objects in the supplementary data (S1 File). The graph densities for all resulting networks were in the same range as the density of the Reactome interaction network (Table 2).

Identification and functional characterization of the most important genes in the reconstructed association networks

The combined topological centrality measure was used to characterize the biological importance of nodes (genes) in the reconstructed association networks. The 5% of the highest ranked genes listed in supplementary S3 Table were mapped to Reactome pathways in order to further evaluate their biological roles. The top 10 most relevant pathways according to the FDR values are shown in Table 3. For the cell line with increased radiation sensitivity after irradiation with 1 Gy and for the normal sensitive cell line after 10 Gy the induction of pathways associated with senescence response was detected. For the cell line with increased radiation sensitivity after 10 Gy of irradiation we mostly observed pathways associated with apoptosis. All pathways are listed in supplementary S4 Table.

False detected differentially expressed genes between technical replicates

In order to assess the false positive rate, the spline regression based differential analyses between technical replicates of each treatment conditions and cell lines were performed. Here, we can state that the null-hypothesis of no differential expression is true for all genes. Then the q^*-level of 0.05 for Benjamini-Hochberg method controls also the FWER at alpha-level equal to 0.05 (type I error) [22]. For all compared technical replicates not more than 3% rejections of null hypothesis were detected, which is in good accordance to the expected or nominal type I error.

Evaluation of spline regression model in comparison to BETR method

Table 1 compares the numbers of differentially expressed genes obtained from both methods applied on the same gene expression data set and FDR thresholds. For almost all treatment conditions the BETR method detected less differentially expressed genes in comparison to

Table 1. Number of detected and differentially expressed genes for each dose and cell lines for NCSRM and BETR methods.

cell line and applied radiation dose	increased sensitivity (1 Gy vs 0 Gy)	Normal sensitivity (1 Gy vs 0 Gy)	increased sensitivity (10 Gy vs 0 Gy)	Normal sensitivity (10 Gy vs 0 Gy)
total number of detected probes after preprocessing	10388	11311	10330	11446
differentially expressed genes detected with **NCSRM**	2335	7	6019	3892
differentially expressed genes detected with **BETR**	923	12	3889	1256
intersection of differentially expressed genes resulting from both methods	855	4	3875	1233

doi:10.1371/journal.pone.0160791.t001

Table 2. Number of genes subjected to GAN reconstruction and properties of resulted GANs.

method	NCSRM				BETR			
cell line and applied radiation dose	Increased sensitivity (1 Gy)	normal sensitivity (1 Gy)	Increased sensitivity (10 Gy)	normal sensitivity (10 Gy)	Increased sensitivity (1 Gy)	normal sensitivity (1 Gy)	Increased sensitivity (10 Gy)	normal sensitivity (10 Gy)
number of genes taken for network reconstruction	2335	7	6019	3892	923	12	3889	1256
number of nodes remained in the network	1140	-	3483	2735	336	-	2299	773
number of edges in the network	12198	-	114629	84695	3268	-	126378	16862
network density	0.00939	-	0.00945	0.01133	0.02903	-	0.02392	0.02826
density of the Reactome interaction network	0.00536							

Gene association network reconstructions were performed using the GeneNet method [18]. Association between two genes was considered as significant if posterior edge probability was equal or greater than 0.95. Densities of the reconstructed networks were compared with the density of the Reactome interaction network in order to assess their complexity.

doi:10.1371/journal.pone.0160791.t002

NCSRM. Only for the normal cell line after irradiation with 1 Gy BETR identified 12 genes whereas NCSRM identified only 7 genes. As a consequence of the lower numbers of detected differentially expressed genes with BETR, the obtained networks are smaller than those obtained after spline regression. The detailed comparison results including numbers of detected differentially expressed genes and the sizes of reconstructed association networks are presented in the Table 2. The lists of differentially expressed genes obtained with the two methods are shown in supplementary S1 Table. The top 10 pathways to which the 5% of the most important genes in the reconstructed association networks where mapped to are shown in Table 3. With NCSRM we were not only able to detect almost all genes that were detected also by BETR (Table 1), but also an additional set of genes resulting in almost twice the number of genes compared to BETR. Nevertheless, the top 5% hub genes of the networks derived from the differentially expressed genes defined by BETR were associated with similar biological processes as those from the spline differential expression analysis derived networks. The numbers and names of overlapping hub genes in the GANs are presented in Table 4 and in supplementary S3 Table, respectively.

Evaluation of reconstructed networks

The evaluation of the two networks derived after 1 Gy irradiation of the cell line with increased sensitivity showed that the network reconstructed with the differentially expressed genes determined using BETR did not contain significantly more common edges than random networks ($p = 0.529$), whereas the network reconstructed with the differentially expressed genes determined by NCSRM did ($p = 0.048$). The networks derived after 10 Gy irradiation of the cell line with increased sensitivity and 10 Gy irradiation of the normal sensitive cell line contained significantly more edges that were common with the Reactome network compared to random networks for both methods.

Discussion

The success of tumor radiation therapy predominantly depends on the total applied radiation dose, but also on the tolerance of the tumor surrounding normal tissues to radiation. Toxicity

Table 3. Comparison of NCSRM and BETR methods with respect to the top 10 pathways after mapping of 5% highest ranked genes from the reconstructed gene association networks.

with NCSRM method			with BETR method		
increased sensitivity (1 Gy)	**increased sensitivity (10 Gy)**	**normal sensitivity (10 Gy)**	**increased sensitivity (1 Gy)**	**increased sensitivity (10 Gy)**	**normal sensitivity (10 Gy)**
Signal Transduction	Signal Transduction	Generic Transcription Pathway	DNA Damage/Telomere Stress Induced Senescence[a]	Activation of BH3-only proteins[b]	DNA Damage/ Telomere Stress Induced Senescence[a]
Cellular Senescence[a]	Activation of BH3-only proteins[b]	DNA Damage/ Telomere Stress Induced Senescence[a]	Senescence-Associated Secretory Phenotype (SASP)[a]	Activation of PUMA and translocation to mitochondria[b]	Generic Transcription Pathway
DNA Damage/ Telomere Stress Induced Senescence[a]	Activation of PUMA and translocation to mitochondria[b]	Immune System	Signal Transduction	Cytokine Signaling in Immune system	Cellular Senescence[a]
Formation of Senescence-Associated Heterochromatin Foci (SAHF)[a]	Fatty acid, triacylglycerol, and ketone body metabolism	Gene Expression	Activated PKN1 stimulates transcription of AR (androgen receptor) regulated genes KLK2 and KLK3	Immune System	Gene Expression
Cellular responses to stress	Metabolism	Inositol phosphate metabolism	Cell Cycle Checkpoints	Intrinsic Pathway for Apoptosis[b]	Meiotic recombination
RAF-independent MAPK1/3 activation	Metabolism of proteins	IRF3-mediated induction of type I IFN	Cellular Senescence[a]	Signal Transduction	Signal Transduction
Signaling by ERBB4	PPARA activates gene expression	Cellular Senescence[a]	DNA methylation	Gene Expression	Cell Cycle
DAP12 interactions	Regulation of lipid metabolism by Peroxisome proliferator-activated receptor alpha (PPARalpha)	Formation of Senescence-Associated Heterochromatin Foci (SAHF)[a]	Packaging Of Telomere Ends	BH3-only proteins associate with and inactivate anti-apoptotic BCL-2 members[b]	Transcriptional activation of cell cycle inhibitor p21
PRC2 methylates histones and DNA	Activation of gene expression by SREBF (SREBP)	STING mediated induction of host immune responses	RNA Polymerase I Promoter Opening	Activation of the mRNA upon binding of the cap-binding complex and eIFs, and subsequent binding to 43S	Transcriptional activation of p53 responsive genes
Apoptotic execution phase[b]	BH3-only proteins associate with and inactivate anti-apoptotic BCL-2 members[b]	Metabolism	SIRT1 negatively regulates rRNA Expression	Endosomal/Vacuolar pathway	Senescence-Associated Secretory Phenotype (SASP)[a]

[a]Pathways associated with senescence responses.

[b]Pathways associated with apoptotic processes.

doi:10.1371/journal.pone.0160791.t003

towards radiation, which greatly varies on an individual level due to inherited susceptibility, is one of the most important limiting factors for dose escalation in radiooncology treatment [23, 24]. To account for radiation sensitivity of normal tissue in personalized treatment approaches the underlying molecular mechanisms need to be thoroughly understood in order to identify

Table 4. Comparison of hub genes in networks resulting from different methods.

cell line and applied radiation dose	increased sensitivity (1 Gy)	increased sensitivity (10 Gy)	Normal sensitivity (10 Gy)
5% hub genes in the NCSRM resulting network in numbers	57	174	137
5% hub genes in the BETR resulting network in numbers	17	115	39
number of common hub genes resulting from both methods	9	111	31

doi:10.1371/journal.pone.0160791.t004

molecular targets for the modulation of radiation sensitivity and molecular markers for the stratification of patients with different intrinsic radiation sensitivity. In the present study we identified significantly differentially expressed genes over time between the radiation-treated group and the control group to be used as prior genes for GAN reconstruction. Two doses of gamma irradiation were used to characterize the differences in radiation response of the two lymphoblastoid cell lines with known differences in radiation sensitivity. The dose of 10 Gy was selected following the fact that the same dose has been applied in a previous research project examining the radiation sensitivity of the same lymphoblastoid cell lines analyzed in the study at hand [20]. The dose of 1 Gy reflects the dose that is delivered as part of the so called "low-dose bath" to the tumor-surrounding tissue during the radiotherapy of the tumors [25].

Here, we conducted time-resolved transcriptome analysis of radiation-perturbed cell culture models of non-tumor cells with normal and with increased radiation sensitivity in order to work out the molecular phenotype of radiation sensitivity in normal cells. Moreover, we present an innovative approach for the identification of GANs from time-course perturbation transcriptome data. The approach comprises three major steps: 1) the identification of differentially expressed genes from time-course gene expression data by employing a natural cubic spline regression model (NCSRM); 2) the use of a regularized dynamic partial correlation method to infer gene associations network from differentially expressed genes; 3) the identification and functional characterization of the key nodes (hubs) in the reconstructed gene dependency network (Fig 1).

Our proposed method for the detection of differentially expressed genes over time is based on NCSRM with a small number of basis functions. A relatively low number of basis functions generally results in a good fit of data and, at the same time, reduces the complexity of the fitted models. Treating time in the model as a continuous variable, a non-linear behavior of gene expressions was approximated by spline curves fitted to the experimental time-course data. Considering temporal changes in gene expression as continuous curves and not as single time points greatly decreases the dimensionality of the data and thereby decreases computational cost. In addition, the proposed NCRSM does not require identical sampling time points for the compared treatment conditions. Furthermore, no biological replicates are needed. Therefore, the method is applicable to data generated according to a tailored time-course differential expression study design and to data that were not specifically generated for time-course differential expression analysis, e.g. existing/previously generated data from clinical samples. Thus, the adaption of the method to differential expression analysis comprises the potential to reanalyze existing data, address new questions *in silico* and thereby potentially add new or additional value to existing data. Incomplete time-course data, e.g. due to the exclusion of samples for technical reasons, that often create major problems for the estimation of the model, are also suitable for fitting the spline regression model as long as enough data points remain in the data set. This is especially valuable when data on certain time points, derived from a very limited sample source, have been excluded from a time-course data set and cannot be repeatedly generated.

Since gene expression is not only dynamic in the treatment group but also in the control group, the inclusion of the time-course control data greatly improves the ability to detect truly differentially expressed genes, as the gene expression values are not referred to a single time point with static gene expression levels only. Comparing a treatment group to time point zero does not provide a proper control over the entire time-course, although it is widely practiced [26–28]. The proposed workflow is implemented in an open-source R-package splineTimeR and is available through Bioconductor (https://www.bioconductor.org).

Amongst a panel, the two lymphoblastoid cell lines that were different with regard to radiation sensitivity after irradiation with 10 Gy [20], also responded differently with regard to the

quantity of differentially expressed genes. Interestingly, cells with normal radiation sensitivity barely responded to 1 Gy irradiation at the transcriptome level. Only seven genes (FDXR, BBC3, VWCE, PHLDA3, SCARF2, HIST1H4C, PCNA) were identified as differentially expressed, whereas for the cell line with increased sensitivity 2335 differentially expressed genes were detected after exposure to the same dose. A similar behavior was observed for those two cell lines after irradiation with 10 Gy. We detected 6019 and 3892 genes as differentially expressed in the sensitive and normal cell lines, respectively (Table 2). Those results are in a good agreement with the previous proteomic study where more differentially expressed proteins were detected for the same sensitive cell line compare to the cell line with normal radiation sensitivity 24 hours after irradiation with 10 Gy [29]. Thus, for both applied doses, the radiation sensitive cells exhibited much more pronounced transcriptional response compared to the cells with normal radiation sensitivity and thereby underlines the expected radiation response of those two cell lines.

Concerning qualitative differences in the transcriptomic response of normal sensitive cells and cells with increased sensitivity after treatment with 1 Gy and 10 Gy pathway enrichment analysis was performed. Differentially expressed genes identified for all considered treatment conditions except for the normal sensitive cells after exposure to 1 Gy radiation showed statistically significant enrichment of pathways. Most of which were in agreement with known radiation responses such as DNA repair, cell cycle regulation, oxidative stress response or pathways related to apoptosis (S2 Table) [30–32]. Therefore, the pathway enrichment analysis results suggest plausibility of generated data and, more importantly, underline the meaningfulness of our suggested approach based on cubic spline regression for differential gene expression analysis of time-course data. However, differential expression analysis alone followed by pathway enrichment analysis does not provide any mechanistic insights. For this reason we performed GAN reconstruction using identified differentially expressed genes. Based on the assumption that the expression levels of functionally related genes are highly correlated, partial correlation was used for GAN reconstruction. In simple correlation, the strength of the linear relationship between two genes is measured, without taking into account that those genes may be actually influenced by other genes. Partial correlation eliminates the influence of other genes when one particular relationship between pair of genes is considered. Network reconstruction was performed separately for the cell line with increased radiation sensitivity after 1 Gy and 10 Gy and for the cell line with normal radiation sensitivity after 10 Gy of radiation dose. Due to the sparseness of the set of genes differentially expressed after irradiation of the normal-sensitive cell line with 1 Gy, no GAN was obtained.

Subsequently, we identified the network hubs (i.e. most important genes) of the GANs by combining three network centrality measures: degree, closeness and shortest path betweenness [33]. Combining different centrality measures is a widely used approach to identify nodes that are likely to control the network [34]. Also, this approach allows identification of nodes that are connected to the central nodes at the same time which can be informative for the interpretation of the whole GAN or single modules making up the network [33, 34].

Identification of key pathways associated with radiation sensitivity

In order to get functional insights into the reconstructed GANs the 5% top important nodes were identified after a ranking with the combined centrality measure and mapped to the pathways from the interactome database Reactome [35]. The obtained results revealed different pathways considered as the most important in cells with different radiation sensitivity after different doses of ionizing radiation. For the radiation sensitive cell line 4060–200 and 1 Gy irradiation, we mainly detected pathways associated with senescence (Table 3).

A different outcome was observed after irradiation with 10 Gy. For the radiation sensitive cells three out of the ten top pathways were linked to apoptotic processes with the genes BBC3, BCL2, TP53 as key players, whereas for the normal sensitive cell line we mainly observed the induction of senescence related pathways. This indicates that different doses are necessary to induce a similar response in the two cell lines. The activation of senescence genes is a damage response mechanism, which stably arrests proliferating cells and protects them from apoptotic cell death [36]. Together with the senescence pathway we observed increased levels of chemokine, cytokine and interleukin genes that are known to activate an immune response and signal transduction pathways in response to irradiation.

Although the senescence-associated pathways were not seen as the most important ones for the treatment condition 10 Gy/increased sensitivity, they were significantly enriched in the GANs of the three conditions 1 Gy/increased sensitivity, 10 Gy/ increased sensitivity and 10 Gy/normal sensitivity. All differentially expressed genes that related to senescence-associated pathways are shown in supplementary S5 Table. The observation that cells with increased radiation sensitivity compared to cells with normal sensitivity, become senescent after exposure to doses in the range of 1 Gy, rises the question whether this has a positive or negative influence on the tumor therapy. On the one hand side, senescent cell may secret the so-called SASP ("senescence-associated secretory phenotype") factors, including growth factors, chemokines and cytokines, which participate in intercellular signaling leading to the attraction of immune cells to the tumor location that, in turn, eliminate the tumor cells and, thereby, positively contribute to the tumor therapy [37, 38]. On the other hand side, senescent cells and the SASP are reported to promote proliferation, survival, invasion and migration of neighboring cells by the release of pro-inflammatory cytokines leading to sustained inflammation [36]. In this way senescence cells can damage their local environment and stimulate angiogenesis and tumor progression [39, 40]. Besides, there are some evidences that the induction of senescence in surrounding normal tissue may lead to an increased radio-tolerance or even radioresistance of the tumor and is, therefore, not desirable and negatively influences the tumor radiotherapy [41]. Thus, it might be beneficial to block senescence in order to prevent the radio-hyposensibilization of tumor cells. Therefore, we suggest a detailed investigation of the consequences of senescent non-tumor cells with the aim to improve the radiotherapy of tumors in radiosensitive patients.

Identification of senescence associated genes involved in cell radiation responses

CDKN1A gene was identified as one of the most important key players linked to the identified senescence associated pathways for both 1 Gy/sensitive and 10 Gy/normal treatment conditions. For both conditions the expression of the CDKN1A was up-regulated for all considered time points. CDKN1A is a well-known damage response gene for which aberrant transcriptional response has been associated with abnormal sensitivity to ionizing radiation [42, 43]. The study by Badie et al. (2008) has shown that a subgroup of breast cancer patients, who developed severe reactions to radiation therapy, could be identified by aberrant overexpression of CDKN1 in peripheral blood lymphocytes [43].

LMNB1 is another genes we identified as a response hub gene after irradiation of sensitive cell line with 1 Gy radiation dose that is associated with senescence. Although the LMNB1 gene was not identified as hub gene in the GAN of the 10 Gy/normal treatment condition, it was still differentially expressed. For both treatment conditions we observed significant downregulation of this gene 24 hours after irradiation. Shah et al (2013) has suggested that downregulation of LMNB1 in senescence is a key trigger of chromatin changes affecting gene expression [44]. In fact also in our data we observed strong downregulation of a group of histone genes associated

with senescence (S5 Table) for the treatment conditions 1 Gy/increased sensitivity and 10 Gy/normal sensitivity. Furthermore, Lee et al. (2012) has shown that histone protein modification may have an impact on the radiation sensitivity of a tissue [45]. Moreover, evidence has been provided that mutation of LMNA can cause increased sensitivity to ionizing radiation [46], however, to our knowledge there are no data showing the role of LMNB gene in the context of radiation sensitivity.

Another potential therapeutic candidate associated with senescence that was identified for the 10 Gy/normal sensitivity treatment condition was MRE11A for which cell culture data suggest that treatment of cells with Mre11 siRNA increases radiation sensitivity and reduces heat-induced radiosensitization [47, 48]. However, the clinical applicability of MRE11, has not been confirmed [49].

Assessment of the false positive rate and validation of the NCSRM method

The spline regression based differential analyses between technical replicates were performed in order to estimate the extent of random fluctuations of gene expression values. The detected 3% rejections of the overall null hypothesis of no differential gene expression are in accordance with the alpha-level of 5% of the familywise error rate (FWER) and can be considered as false positives. On the other hand, it shows that type I error, due to technical variation, is covered by the model and test assumptions (moderated F-test, [50]) so that it was not necessary to include an extra parameter for technical replicates into the model.

In order to validate the previously mentioned biological results using NCSRM, we performed the differential expression analysis with another established method for time-course data analysis called BETR (Bayesian Estimation of Temporal Regulation) [6]. The number of genes detected by BETR was considerably lower compared to NCRSM (Table 1), however the majority of which were also detected with NCSRM (S1 Table). This is in line with the calculations on the false positive rates that have been conducted on the simulated data presented in the BETR study. In an analysis of the simulated data set, 65% of truly differentially expressed genes have been identified after accepting a false positive rate of 5% [6]. This means that a substantial proportion of differentially expressed genes remained undetected, which is likely to be also the case for the herein analyzed data with BETR. Although the numbers of differentially expressed genes and genes remained in the reconstructed networks greatly differ (Table 1), the qualitative results are well comparable (Table 3). For all treatment conditions where for which we were able to reconstruct GANs, we observed a great overlap of pathways where the 5% of hub genes were mapped to (Table 3). The detection of a higher number of differentially expressed genes with NCSRM resulted in larger GANs with additional information compared to the smaller GANs that were reconstructed on the basis of genes detected with BETR. This is underlined by the results of the conducted evaluation of GANs. Except one network based on the differentially expressed genes using BETR, all investigated networks consist significantly more common edges with the Reactome reference network compared to random networks with identical network topology and genes. This shows that the additionally detected genes with NCSRM add additional information rather than adding false positives or noise to the set of differentially expressed genes. Moreover the spline regression method is much more flexible and allows for more freedom during the data collection process. As already mentioned, NCSRM does not require the same sampling time for treated and control groups and can easily deal with incomplete data, whereas BETR method is not able to overcome or bypass those limitations. Thus, NCSRM is very robust against the frequently occurring shortcomings in study design and subsequent data generation occurring in life sciences.

Conclusion

Prospectively, we suggest and plan a detailed *in silico* and *in vitro* analysis of the interactions in the proposed gene association networks in order to add meaningful knowledge to the mechanism of radiosensitivity at the experimental level. This novel knowledge has the potential to improve cancer radiation therapy by preventing or lowering the acute responses of normal cells resulting from radiation therapy. The results add novel information to the understanding of mechanisms that are involved in the radiation response of human cells, with the potential to improve tumor radiotherapy. Besides, the presented workflow is not limited to presented study only, but may be applied in other special fields with different biological questions to be addressed.

The software is provided as R-package "splineTimeR" and freely available via the Bioconductor project at http://www.bioconductor.org.

Material and Methods

Cell culture

Experiments were conducted with two monoclonal lymphoblastoid Epstein-Barr virus-immortalized cell lines (LCL) obtained from young lung cancer patients of the LUCY study (**LU**ng **C**ancer in **Y**oung) that differ in radiosensitivity, as tested with Trypan Blue and WST-1 assays [19, 20]. The non-cancer cell lines LCL 4060–200 with increased radiation sensitivity and LCL 20037–200 with normal radiation sensitivity were cultured at 37°C/5% CO_2 in RPMI 1640 medium (Biochrom) supplemented with 10% fetal calf serum (FCS; PAA). Mycoplasma contamination was routinely tested using luminescence-based assays (MycoAlert, Lonza).

Irradiation and sample preparation

The cells were seeded in 75 cm^2 flasks at a concentration of 0.5 x 10^6 cells/ml in a total volume of 60 ml. Exponentially growing cells were irradiated with sham, 1 Gy and 10 Gy of gamma-irradiation (^{137}Cs-source HWM-D 2000, Markdorf, Germany) at a dose rate of 0.49 Gy/min. Samples were collected 0.25, 0.5, 1, 2, 4, 8 and 24 hours after sham or actual irradiation. Between the time of collection cells were kept in the incubator. Collected cells were washed with PBS and frozen at -80°C. Total RNA was isolated from frozen cell pellets obtained from two independent experiments using the AllPrep DNA/RNA/miRNA Universal Kit (Qiagen) including an DNase digestion step, according to the manufacturer's protocol. The concentration of RNA was quantified with a Qubit 2.0 Fluorometer (Life Technologies), and integrity was determined using a Bioanalyzer 2100 (Agilent Technologies). RNA samples with a RNA integrity number (RIN) greater than 7 indicated sufficient quality to be used in subsequent RNA microarray analysis.

Gene expression profiling

Transcriptional profiling was performed using SurePrint G3 Human Gene Expression 8x60k V2 microarrays (Agilent Technologies, AMADID 39494) according to the manufacturer's protocol. 75 ng of total RNA was used in labeling using the Low Input Quick Amp Labeling Kit (one-color, Agilent Technologies). Raw gene expression data were extracted as text files with the Feature Extraction software 11.0.1.1 (Agilent Technologies). The expression microarray data were uploaded to ArrayExpress (www.ebi.ac.uk/arrayexpress/) and the data set is available under the accession number E-MTAB-4829. All data analysis was conducted using the R statistical platform (version 3.2.2, www.r-project.org) [51]. Data quality assessment, filtering, preprocessing, normalization, batch correction based on nucleic acid labeling batches and data

analyses were carried out with the Bioconductor R-packages limma, Agi4x44PreProcess and the ComBat function of the sva R-package [4, 21, 52]. All quality control, filtering, preprocessing and normalization thresholds were set to the same values as suggested in Agi4x44PreProcess R-package user guide [21]. Only HGNC annotated genes were used in the analysis. For multiple microarray probes representing the same gene the optimal probe was selected according to the Megablast score of probe sequences against the human reference sequence (http://www.ncbi.nlm.nih.gov/refseq/) [53]. If the resulted score was equal for two or more probes, the probe with the lowest differential gene expression FDR value was kept for further analyses since only one expression value per gene was allowed in subsequent GAN reconstruction analysis.

Spline regression model for two-way experimental design

A natural cubic spline regression model (NCSRM) with three degrees of freedom for an experimental two-way design with one treatment factor and time as a continuous variable was fitted to the experimental time-course data. The mathematical model is defined by the following eq (1):

$$\begin{aligned} y &= y(t,x) \\ &= b_0 + b_1 B_1(t-t_0) + b_2 B_2(t-t_0) + \ldots + b_m B_m(t-t_0) + x(d_0 + d_1 B_1(t-t_0) + d_2 B_2(t \\ &\quad - t_0) + \ldots + d_m B_m(t-t_0)) \end{aligned}$$

where $b_0, b_1, \ldots, b_m$ are the spline coefficients in the control group and $d_0, d_1, \ldots, d_m$ are differential spline coefficients between the control and the irradiated group. $B_1(t\text{-}t_0)$, $B_2(t\text{-}t_0)$, $\ldots$, $B_m(t\text{-}t_0)$ are the spline base functions and t_0 is the time of the first measurement. For x = 0, $y = y_{control}$ and for x = 1, $y = y_{irradiated}$. For three degrees of freedom (df = 3), m = 3.

Depending on the number of degrees of freedom, two boundary knots and df-1 interior knots are specified. The interior knots were chosen at values corresponding to equally sized quantiles of the sampling time from both compared groups. For example, for df = 3 interior knots correspond to the 0.33- and 0.66-quantiles. The spline function is cubic on each defined by knots intervals, continuous at each knot and has continuous derivatives of first and second orders.

Time-course differential gene expression analysis

The time-course differential gene expression analyses were conducted between irradiated and control cells (sham-irradiated). Analyses were performed on the normalized gene expression data using NCSRM with three degrees of freedom. The splines were fitted to the real time-course expression data for each gene separately according to eq (1). The example of spline regression model fitted to the measured time-course data for one selected gene is shown on the Fig 2.

Time dependent differential expression of a gene between the irradiated and corresponding control cells was determined by the application of empirical Bayes moderated F-statistics [50] on the differential coefficients values in eq (1). In order to account for the multiple-testing error, corresponding p-values were adjusted by the Benjamini-Hochberg method for false discovery [22]. Genes with an adjusted p-value (FDR, false discovery rate) lower than 0.05 were considered as differentially expressed and associated with radiation response.

Assessment of the false positive rate of the NCSRM

Additionally, in order to assess the false positive rate (statistical type I error, also called familywise error rate or FWER) we applied differential gene expression analysis using NCSRM between two technical replicates for all treatment groups. Because only two technical replicates were generated for each time point and treatment, we could not use the same approach to assess the technical variability for the BETR method, as it requires at least two replicates in each compared groups.

Gene association network reconstruction from prior selected differentially expressed genes

Differentially expressed genes were subjected to gene association network reconstruction from time-course data using a regularized dynamic partial correlation method [54]. Pairwise relationships between genes over time were inferred based on a dynamic Bayesian network model with shrinkage estimation of covariance matrices as implemented in the GeneNet R-package available from CRAN [18]. Analyses were conducted with a posterior probability of 0.95 for each potential edge. Edge directions were not considered. In order to assess the complexity of the resulting networks, the density of each network was compared to the density of the Reactome functional interaction network [35, 55].

Identification of important nodes in the network

Graph topological analyses based on centrality measures were applied in order to determine the importance of each node in the reconstructed association networks [56]. Three most

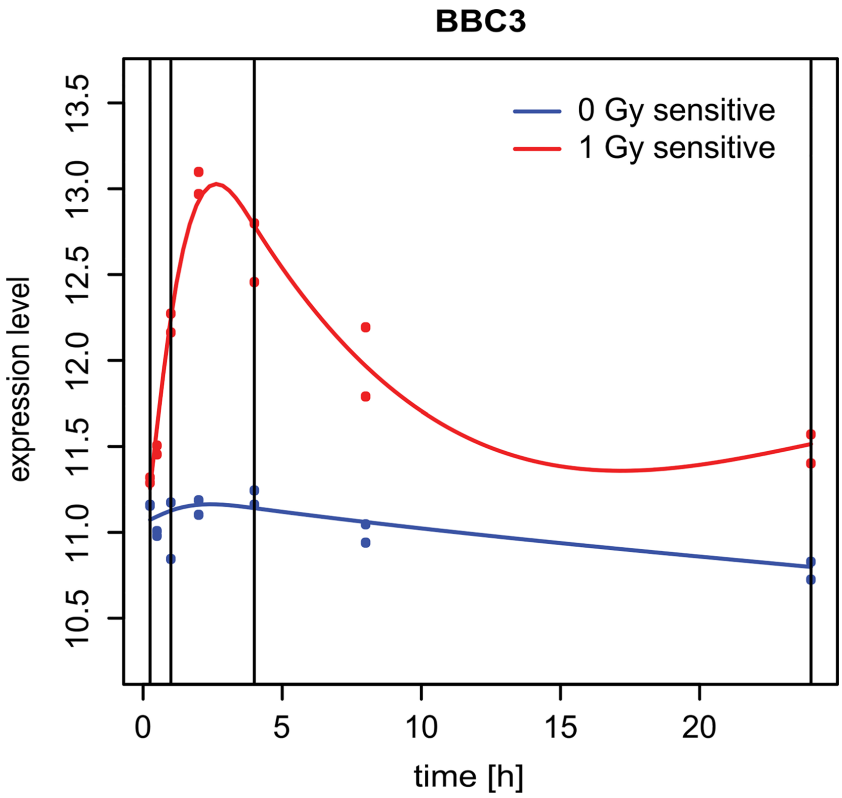

Fig 2. Example of fitted spline regression models. The plot shows spline regression models fitted to the measured time-course expression data of an arbitrary chosen gene (BBC3). The blue line represents the fitted model for the control (0 Gy) and read line that for the irradiated group (1 Gy). Blue and red dots represent the measured expression levels of the biological replicates. Vertical lines represent the endpoints and interior knots correspond to the 0.33- and 0.66-quantiles.

doi:10.1371/journal.pone.0160791.g002

commonly used centrality measures: degree, shortest path betweenness and closeness were combined into one cumulative centrality measure [34]. For each gene the three centrality values where ranked. The consensus centrality measure for each node was defined as the mean of the three independent centrality ranks. Combining centrality measures supports the identification of the nodes that are central themselves and also connected to direct central nodes, which demonstrates strategic positions for controlling the network.

Pathway enrichment analysis

The Reactome pathway database was used to conduct the pathway enrichment analysis in order to further investigate the functions of the selected sets of differentially expressed genes [35]. Statistical significance of enriched pathways was determined by one-sided Fisher's exact test. The resulting p-values were adjusted for FDR using the Benjamini-Hochberg method. Pathways with FDR$<$0.05 were considered statistically significant and pathways were ranked according to ascending FDRs.

Evaluation of NCSRM approach

Since we decided to use the set of genes that appeared to be differentially expressed we assessed the performance of the herein used NCSRM approach in comparison to the BETR approach implemented in the R/Bioconductor package betr [6]. BETR is a well-established algorithm that has been previously compared to limma, MB-statistic and EDGE methods and showed the best performance [6]. The results of spline and BETR methods were compared using the same initial microarray gene expression data set. The probabilities of each gene to be differentially expressed obtained with BETR method, were transformed to p-values as described in the original paper. Genes were considered significantly differentially expressed if the Benjamini-Hochberg adjusted p-value was lower than 0.05 (FDR$<$0.05). This transformation allowed us to compare the outcomes of both methods based on the FDR values for differential expression. The resulting differentially expressed genes using BETR were analyzed and subjected to network reconstruction as described above for the differentially expressed genes obtained using NCSRM. Outcomes of both obtained association networks were compared to each other and to the *a priori* known biological network provided by the Reactome database [35].

Evaluation of reconstructed gene association networks

In order to assess the quality of the *de novo* reconstructed gene association networks (GANs), we developed a novel method that compares the interactions in the reconstructed network to the experimentally validated interactions present in the Reactome interaction network. For this purpose we used the Reactome reference network, consisting of protein-protein interaction pairs stored in the Reactome database (http://www.reactome.org/pages/download-data/). For the comparison, sub-networks of reconstructed networks consisting only of genes overlapping with the Reactome network were built. The number of common edges between these two sub-networks was determined and referred to the total number of edges in the reconstructed network (percentage of common edges in the reconstructed network). Further, a permutation test was performed to assess whether the number of common edges in the reconstructed network was significantly higher than in randomized networks with the same genes. Random networks were generated by permutation of the node names in the network, while preserving the reconstructed sub-network topology. After each permutation (n = 1000) the number of common edges with the reference Reactome sub-network was determined. The reconstructed network was considered significantly better than random, if more than 90% of the random sub-networks contained lower numbers of edges common with the Reactome network than the

reconstructed sub-network (p-value < 0.1). All networks reconstructed with the genes determined as differentially expressed from the herein presented spline regression method and the BETR method were evaluated.

Supporting Information

S1 File. Reconstructed gene association networks. All obtained gene association networks are provided as R-objects of type igraph.
(RDATA)

S1 Table. Lists of differentially expressed genes. Table includes differentially expressed genes identified by spline regression and BETR methods. Additionally, a list of overlapping differentially expressed genes between both methods is included.
(XLSX)

S2 Table. Lists of significantly enriched pathways using differentially expressed genes identified by spline regression method. Four lists of significantly enriched pathways correspond to each used treatment condition. Lists include total numbers of known genes in the pathways, numbers of differentially expressed genes that belong to a single pathway (matches), percentages of differentially expressed genes in comparison to the total number of know genes in the pathway (% match), p-values, FDRs and names of pathways related differentially expressed genes.
(XLSX)

S3 Table. Lists of 5% of most important genes identified by centrality measures. Lists of 5% highest ranked genes from the reconstructed gene association networks using spline regression and BETR methods. Overlap represents common most important genes identified in networks from compared methods.
(XLSX)

S4 Table. Lists of pathways after mapping of 5% highest ranked genes from the reconstructed gene association networks. Lists include names of pathways together with names of mapped most important genes.
(XLSX)

S5 Table. Significantly enriched senescence associated pathways with corresponding differentially expressed genes. Table presents the names of significantly enriched (FDR$<$0.05) senescence associated pathways with corresponding differentially expressed genes for all treatment conditions.
(XLSX)

Acknowledgments

We thank Aaron Selmaier from the Research Unit Radiation Cytogenetics for technical support. This study was supported by the Federal Ministry of Education and Research, ZiSS project, 02NUK024B.

Author Contributions

Conceived and designed the experiments: AD AM KU HZ NB JH MG SH.

Performed the experiments: AM AD.

Analyzed the data: AM HB MS.

Contributed reagents/materials/analysis tools: AM AD MS KU MG SH HZ.

Wrote the paper: AM KU MS.

Biological data interpretation: AM KU HZ JH MS MG SH NB. Designed the software used in analysis: AM HB. Revision of the manuscript: KU HZ JH MG SH NB AD HB. Final approval of the version to be published: AM HB MS AD JH MG SH NB HZ KU.

References

1. Bar-Joseph Z, Gitter A, Simon I. Studying and modelling dynamic biological processes using time-series gene expression data. Nature Reviews Genetics. 2012; 13:552–64. doi: 10.1038/nrg3244 PMID: 22805708
2. Bandyopadhyay S, Bhattacharyya M. A biologically inspired measure for coexpression analysis. IEEE/ACM Transactions on Computational Biology and Bioinformatics. 2011; 8(4):929–42. doi: 10.1109/TCBB.2010.106 PMID: 21566252
3. Yuan M, Kendziorski C. Hidden Markov models for microarray time course data in multiple biological conditions. Journal of the American Statistical Association. 2006; 101(476):1323–32.
4. Smyth GK. Limma: linear models for microarray data. In: 'Bioinformatics and Computational Biology Solutions Using {R} and Bioconductor'. New York: Springer, p. 397–420; 2005.
5. Leek JT, Monsen E, Dabney AR, Storey JD. EDGE: extraction and analysis of differential gene expression. Bioinformatics. 2006; 22(4):507–8. PMID: 16357033
6. Aryee MJ, Gutiérrez-Pabello JA, Kramnik I, Maiti T, Quackenbush J. An improved empirical bayes approach to estimating differential gene expression in microarray time-course data: BETR (Bayesian Estimation of Temporal Regulation). BMC Bioinformatics. 2009; 10(409).
7. Conesa A, Nueda MJ, Ferrer A, Talón M. maSigPro: a method to identify significantly differential expression profiles in time-course microarray experiments. Bioinformatics. 2006; 22(9):1096–102. PMID: 16481333
8. Ernst J, Bar-Joseph Z. STEM: a tool for the analysis of short time series gene expression data. BMC Bioinformatics. 2006; 7(191).
9. Schliep A, Steinhoff C, Schönhuth A. Robust inference of groups in gene expression time-courses using mixtures of HMMs. Bioinformatics. 2004; 20:i283–i9. PMID: 15262810
10. Magni P, Ferrazzi F, Sacchi L, Bellazzi R. TimeClust: a clustering tool for gene expression time series. Bioinformatics. 2008; 24(3):430–2. PMID: 18065427
11. Sivriver J, Habib N, Friedman N. An integrative clustering and modeling algorithm for dynamical gene expression data. Bioinformatics. 2011; 27(13): i392–i400. doi: 10.1093/bioinformatics/btr250 PMID: 21685097
12. Sinha A, Markatou M. A Platform for Processing Expression of Short Time Series (PESTS). BMC Bioinformatics. 2011; 12(13).
13. Ramoni MF, Sebastiani P, Kohane IS. Cluster analysis of gene expression dynamics. Proc Natl Acad Sci USA. 2002; 99:9121–6. PMID: 12082179
14. Lin T, Kaminski N, Bar-Joseph Z. Alignment and classification of time series gene expression in clinical studies. Bioinformatics. 2008; 24:i147–i55. doi: 10.1093/bioinformatics/btn152 PMID: 18586707
15. Costa IG, Schönhuth A, Hafemeister C, Schliep A. Constrained mixture estimation for analysis and robust classification of clinical time series. Bioinformatics. 2009; 25:i6–i14. doi: 10.1093/bioinformatics/btp222 PMID: 19478017
16. Hafemeister C, Costa IG, Schönhuth A, Schliep A. Classifying short gene expression time-courses with Bayesian estimation of piecewise constant functions. Bioinformatics. 2011; 27(7):946–52. doi: 10.1093/bioinformatics/btr037 PMID: 21266444
17. Storey JD, Xiao W, Leek JT, Tompkins RG, Davis RW. Significance analysis of time course microarray experiments. PNAS. 2005; 102(36):12837–42. PMID: 16141318
18. Opgen-Rhein R, Strimmer K. From correlation to causation networks: a simple approximate learning algorithm and its application to high-dimensional plant gene expression data. BMC Syst Biol. 2007; 1:37. PMID: 17683609
19. Rosenberger A, Rossler U, Hornhardt S, Sauter W, Bickeboller H, Wichmann HE, et al. Validation of a fully automated COMET assay: 1.75 million single cells measured over a 5 year period. DNA Repair (Amst). 2011; 10(3):322–37.

20. Guertler A, Kraemer A, Roessler U, Hornhardt S, Kulka U, Moertl S, et al. The WST survival assay: an easy and reliable method to screen radiation-sensitive individuals. Radiat Prot Dosimetry. 2011; 143 (2–4):487–90. doi: 10.1093/rpd/ncq515 PMID: 21183542

21. Lopez-Romero P. Agi4x44PreProcess: PreProcessing of Agilent 4x44 array data. R package version 1.16.0.

22. Benjamini Y, Hochberg Y. Controlling the false discovery rate: a practical and powerful approach to multiple testing. Journal of the Royal Statistical Society. 1995; 57:289–300.

23. Alsner J, Andreassen CN, Overgaard J. Genetic markers for prediction of normal tissue toxicity after radiotherapy. Seminars in Radiation Oncology. 2008; 18:126–35. doi: 10.1016/j.semradonc.2007.10.004 PMID: 18314067

24. Andreassen CN. Can risk of radiotherapy-induced normal tissue complications be predicted from genetic profiles? Acta Oncologica. 2005; 44:801–15. PMID: 16332587

25. Liu H, Andrews DW, Evans JJ, Werner-Wasik M, Yu Y, Dicker AP, et al. Plan quality and treatment efficiency for radiosurgery to multiple brain metastases: non-coplanar RapidArc vs. Gamma Knife. Frontiers in Oncology. 2016; 6(26).

26. Pauli A, Valen E, Lin MF, Garber M, Vastenhouw NL, Levin JZ, et al. Systematic identification of long noncoding RNAs expressed during zebrafish embryogenesis. Genome Research. 2012; 22:577–91. doi: 10.1101/gr.133009.111 PMID: 22110045

27. Lienau J, Schmidt-Bleek K, Peters A, Weber H, Bail HJ, Duda HN, et al. Insight into the molecular pathophysiology of delayed bone healing in a sheep model. Tissue Engineering Part A. 2010; 16 (1):191–9. doi: 10.1089/ten.TEA.2009.0187 PMID: 19678759

28. Schell H, Thompson MS, Bail HJ, Hoffmanna J-E, Schilla A, Dudaa GN, et al. Mechanical induction of critically delayed bone healing in sheep: radiological and biomechanical results. Journal of Biomechanics. 2008; 41(14):3066–72. doi: 10.1016/j.jbiomech.2008.06.038 PMID: 18778822

29. Gürtler A, Hauptmann M, Pautz S, Kulka U, Friedl AA, Lehr S, et al. The inter-individual variability outperforms the intra-individual variability of differentially expressed proteins prior and post irradiation in lymphoblastoid cell lines. Arch Physiol Biochem. 2014; 120(5):198–207. doi: 10.3109/13813455.2014.953548 PMID: 25174346

30. Azzama EI, Jay-Gerinb J-P, Pain D. Ionizing radiation-induced metabolic oxidative stress and prolonged cell injury. Cancer Letters. 2012; 327(1–2):48–60. doi: 10.1016/j.canlet.2011.12.012 PMID: 22182453

31. Li L, Story K, Legerski RJ. Cellular responses to ionizing radiation damage. International Journal of Radiation Oncology, Biology, Physics. 2001; 49(4):1157–62. PMID: 11240259

32. Jung M, Dritschilo A. Signal transduction and cellular responses to ionizing radiation. Seminars in Radiation Oncology. 1996; 6(4):268–72. PMID: 10717184

33. Koschützki D. Network Centralities. In: Junker BH, Schreiber F, editors. Analysis of Biological Networks: Wiley; 2007. p. 65–84.

34. Abbasi A, Hossain L. Hybrid Centrality Measures for Binary and Weighted Networks. In: Menezes R, Evsukoff A, González MC, editors. Complex Networks. 424. Berlin: Springer; 2013. p. 1–7.

35. Matthews L, Gopinath G, Gillespie M, Caudy M, Croft D, de Bono B, et al. Reactome knowledgebase of human biological pathways and processes. Nucleic Acids Res. 2009; 37(Database issue):D619–D22. doi: 10.1093/nar/gkn863 PMID: 18981052

36. Sabin RJ, Anderson RM. Cellular Senescence—its role in cancer and the response to ionizing radiation. Genome Integr 2011; 2: 7 2011; 2(1):7. doi: 10.1186/2041-9414-2-7 PMID: 21834983

37. Meng Y, Efimova EV, Hamzeh KW, Darga TE, Mauceri HJ, Fu YX, et al. Radiation-inducible immunotherapy for cancer: senescent tumor cells as a cancer vaccine. Molecular Therapy. 2012; 20(5):1046–55. doi: 10.1038/mt.2012.19 PMID: 22334019

38. Freund A, Orjalo AV, Desprez PY, Campisi J. Inflammatory networks during cellular senescence: causes and consequences. Trends Mol Med. 2010; 16(5):238–46. doi: 10.1016/j.molmed.2010.03.003 PMID: 20444648

39. Nelson G, Wordsworth J, Wang C, Jurk D, Lawless C, Martin-Ruiz C, et al. A senescent cell bystander effect: senescence-induced senescence. Aging Cell. 2012; 11(2):345–9. doi: 10.1111/j.1474-9726.2012.00795.x PMID: 22321662

40. Wu PC, Wang Q, Grobman L, Chu E, Wu DY. Accelerated cellular senescence in solid tumor therapy. Experimental Oncology. 2012; 34(3):298–305. PMID: 23070015

41. Tsai KK, Stuart J, Chuang YY, Little JB, Yuan ZM. Low-dose radiation-induced senescent stromal fibroblasts render nearby breast cancer cells radioresistant. Radiation Research. 2009; 172(3):306–13. doi: 10.1667/RR1764.1 PMID: 19708779

42. Amundson SA, Grace MB, McLeland CB, Epperly MW, Yeager A, Zhan Q, et al. Human in vivo radiation-induced biomarkers: gene expression changes in radiotherapy patients. Cancer Research. 2004; 64(18):6368–71. PMID: 15374940

43. Badie C, Dziwura S, Raffy C, Tsigani T, Alsbeih G, Moody J, et al. Aberrant CDKN1A transcriptional response associates with abnormal sensitivity to radiation treatment. British Journal of Cancer. 2008; 98(11):1845–51. doi: 10.1038/sj.bjc.6604381 PMID: 18493234

44. Shah PP, Donahue G, Otte GL, Capell BC, Nelson DM, Cao K, et al. Lamin B1 depletion in senescent cells triggers large-scale changes in gene expression and the chromatin landscape. Genes & Development. 2013; 27:1787–99.

45. Lee M, Urata SM, Aguilera JA, Perry CC, Milligan JR. Modeling the influence of histone proteins on the sensitivity of DNA to ionizing radiation. Radiation Research. 2012; 177(2):152–63. PMID: 22103271

46. di Masi A, D'Apice MR, Ricordy R, Tanzarella C, Novelli G. The R527H mutation in LMNA gene causes an increased sensitivity to ionizing radiation. Cell Cycle. 2008; 7(13):2030–7. PMID: 18604166

47. Xu M, Myerson R, Hunt C, Kumar S, Moros E, Straube B, et al. Treatment of cells with Mre11 siRNA increases radiation sensitivity and reduces heat induced radiosensitization. International Journal of Radiation Oncology Biology Physics. 2003; 57(2):144–5.

48. Xu M, Myerson RJ, Hunt C, Kumar S, Moros EG, Straube WL, et al. Transfection of human tumour cells with Mre11 siRNA and the increase in radiation sensitivity and the reduction in heat-induced radiosensitization. International Journal of Hyperthermia. 2004;20(2).

49. Söderlund K, Stål O, Skoog L, Rutqvist LE, Nordenskjöld B, Askmalm MS. Intact Mre11/Rad50/Nbs1 complex predicts good response to radiotherapy in early breast cancer. International Journal of Radiation Oncology Biology Physics. 2007; 68(1):50–8.

50. Smyth GK. Linear models and empirical bayes methods for assessing differential expression in microarray experiments. Statistical Applications in Genetics and Molecular Biology. 2004; 3(1):Article 3.

51. R Core Team. R: A language and environment for statistical computing 2013.

52. Gentleman RC, Carey VJ, Bates DM, Bolstad B, Dettling M, Dudoit S, et al. Bioconductor: open software development for computational biology and bioinformatics. Genome Biol. 2004; 5(10):R80. PMID: 15461798

53. Li Q, Birkbak NJ, Gyorffy B, Szallasi Z, Eklund AC. Jetset: selecting the optimal microarray probe set to represent a gene. BMC Bioinformatics. 2011; 12(474).

54. Opgen-Rhein R, Strimmer K. Using regularized dynamic correlation to infer gene dependency networks from time-series microarray data. The 4th International Workshop on Computational Systems Biology, WCSB. 2006.

55. Wasserman S, Faust K. Social Network Analysis: Methods and Applications: Cambridge: Cambridge University Press; 1994.

56. Koschützki D, Schreiber F. Centrality analysis methods for biological networks and their application to gene regulatory networks. Gene Regulation and Systems Biology. 2008; 2:193–201. PMID: 19787083

Michna et al. Radiation Oncology (2016) 11:94
DOI 10.1186/s13014-016-0672-0

Radiation Oncology

RESEARCH Open Access

Transcriptomic analyses of the radiation response in head and neck squamous cell carcinoma subclones with different radiation sensitivity: time-course gene expression profiles and gene association networks

Agata Michna[1†], Ulrike Schötz[2†], Martin Selmansberger[1], Horst Zitzelsberger[1,3], Kirsten Lauber[2,3], Kristian Unger[1,3] and Julia Hess[1,3*]

Abstract

Background: Acquired and inherent radioresistance of tumor cells is related to tumor relapse and poor prognosis – not only in head and neck squamous cell carcinoma (HNSCC). The underlying molecular mechanisms are largely unknown. Therefore, systemic in-depth analyses are needed to identify key regulators of radioresistance. In the present study, subclones of the CAL-33 HNSCC cell line with different radiosensitivity were analyzed to identify signaling pathways related to the different phenotypes.

Methods: Subclones with altered radiosensitivity were generated by fractionated irradiation of the parental CAL-33 cells. Differences in radiosensitivity were confirmed in colony formation assays. Selected subclones were characterized at the genomic and transcriptomic level by SKY, array CGH, and mRNA-microarray analyses. Time-course gene expression analyses upon irradiation using a natural cubic spline regression model identified temporally differentially expressed genes. Moreover, early and late responding genes were identified. Gene association networks were reconstructed using partial correlation. The Reactome pathway database was employed to conduct pathway enrichment analyses.

(Continued on next page)

* Correspondence: julia.hess@helmholtz-muenchen.de
†Equal contributors
[1]Research Unit Radiation Cytogenetics, Helmholtz Zentrum München, German Research Center for Environmental Health GmbH, 85764 Neuherberg, Germany
[3]Clinical Cooperation Group "Personalized Radiotherapy in Head and Neck Cancer", Helmholtz Zentrum München, 85764 Neuherberg, Germany
Full list of author information is available at the end of the article

(Continued from previous page)

Results: The characterization of two subclones with enhanced radiation resistance (RP) and enhanced radiosensitivity (SP) revealed distinct genomic and transcriptomic changes compared to the parental cells. Differentially expressed genes after irradiation shared by both subclones pointed to important pathways of the early and late radiation response, including senescence, apoptosis, DNA repair, Wnt, PI3K/AKT, and Rho GTPase signaling. The analysis of the most important nodes of the gene association networks revealed pathways specific to the radiation response in different phenotypes of radiosensitivity. Exemplarily, for the RP subclone the senescence-associated secretory phenotype (SASP) together with GPCR ligand binding were considered as crucial. Also, the expression of endogenous retrovirus ERV3-1in response to irradiation has been observed, and the related gene association networks have been identified.

Conclusions: Our study presents comprehensive gene expression data of CAL-33 subclones with different radiation sensitivity. The resulting networks and pathways associated with the resistant phenotype are of special interest and include the SASP. The radiation-associated expression of ERV3-1 also appears highly attractive for further studies of the molecular mechanisms underlying acquired radioresistance. The identified pathways may represent key players of radioresistance, which could serve as potential targets for molecularly designed, therapeutical intervention.

Keywords: Radioresistance, HNSCC, Head and neck cancer, Time-course gene expression, Gene association network, Signaling pathway, Differentially expressed genes, Endogenous retrovirus

Background

Head and neck squamous cell carcinoma (HNSCC) develops in approx. 139,000 individuals per year in Europe with a survival rate of approx. 70 % at 1 year and approx. 40 % at 5 years after therapy [1]. More than 90 % of head and neck cancers are classified as HNSCC and originate from the oral cavity, nasopharynx, oropharynx, hypopharynx, or larynx, respectively [2]. The major risk factors for HNSCC are tobacco smoking, alcohol abuse, and poor oral health [3, 4]. For oropharyngeal cancers, infection with high-risk human papilloma viruses is another important risk factor [5]. Thus, HNSCC is a very heterogeneous cancer entity also in terms of therapy response. Surgical resection followed by radio(chemo)therapy is the standard treatment of HNSCC patient [6, 7]. In locally advanced HNSCC, surgery is often limited by the complex anatomy of the affected region and, therefore, definitive radiochemotherapy is an important treatment option. However, acquired and/or inherent radioresistance of tumor cells is a common cause for tumor relapse and poor prognosis. Tumor cells derived from HNSCCs after radiotherapy have been reported to be more radioresistant than cell lines established prior to therapy, thus strengthening the clinical relevance of acquired radioresistance [8]. Along these lines, it was proposed that fractionated irradiation might preferentially eradicate radiosensitive cells, whereas radioresistant cells remain largely untouched. Accordingly, recurrent tumors mostly consist of radioresistant cells [8]. Although different potential mechanisms of radioresistance have been proposed and extensively studied, the underlying molecular details remain largely unknown [9]. Systemic in-depth analyses are needed in order to identify the master regulators of acquired radioresistance, which could serve as potential biomarkers and future therapeutic targets in novel combined modality approaches.

In this study, we characterized two subclones (#303 and #327) derived from the CAL-33 HNSCC cell line, which were generated by fractionated radiation treatment of the parental cells. CAL-33 is an HPV-negative HNSCC cell line that has been established by Gioanni et al. (1988) from a biopsy specimen prior to treatment from a squamous cell carcinoma of the tongue from a male patient [10]. The subclones derived thereof differed in radiosensitivity when compared to the parental CAL-33 cell line. Interestingly, one subclone was significantly more radioresistant, whereas the other one was significantly more radiosensitive. In order to identify potential key regulators of altered radiation sensitivity, the subclones were characterized on the genomic and transcriptomic level. Furthermore, time-course gene expression analyses were performed upon irradiation, and gene association network reconstruction and pathway enrichment analyses were utilized to identify signaling pathways related to the observed radiation phenotypes.

Methods

Cell culture

The human head and neck squamous cell carcinoma (HNSCC) cell line CAL-33 was obtained from the German collection of microorganisms and cell cultures (DSMZ). Cells were maintained in DMEM GlutaMAX I medium supplemented with 10 % FCS and 1 % penicillin/streptomycin and cultured at 37 °C/5 % CO_2. Cells were mycoplasma-free as tested by the MycoAlert (Lonza) mycoplasma detection kit.

Generation of clones with altered radiation resistance

In order to generate radioresistant subclones of the parental CAL-33 cell line, exponentially growing CAL-33 cells were exposed to fractionated irradiation (Mueller RT-250 γ-ray, tube Thoraeus Filter, 200 kV, 10 mA) according to a schedule commonly used in radiotherapy: A total dose of 20 Gy was given in daily fractions of 2 Gy 5 times per week. For each week, 2 days of recovery time were included. Afterwards, cells were cloned by limiting dilution procedure and grown for 4 to 12 weeks.

Colony forming assay

Clonogenic survival was determined in colony formation assays as described previously [11]. Briefly, cells were seeded into 6-well plates, allowed to adhere for 4 h, and irradiated at 0, 1, 2, 4, 6 or 8 Gy, respectively (Mueller RT-250 γ-ray, Thoraeus Filter, 200 kV, 10 mA). 14 days after irradiation, colonies were fixed and stained with methylene blue. Only colonies consisting of at least 50 cells were scored. Each assay was carried out in duplicates of three different cell densities per each irradiation dose. Results from three independent experiments were subjected to linear-quadratic regression analyses employing the maximum likelihood approach. Differences between curves were evaluated using F-test [12].

Proliferation and cell cycle analyses

Proliferation rates were determined over a period of three days upon seeding 20,000 cells per well into 24-well plates. Cells were harvested by trypsinization, and total cell numbers were determined by manual counting. Cell numbers were plotted against the growth time, and doubling times were calculated by semi-log regression analyses in the exponential growth phase. Dynamics of cell cycle distribution upon irradiation at 4 Gy was analyzed by flow cytometric phospho-histone H3(S10)/propidium iodide (PI) staining as described in [13]. Briefly, cells were collected by trypsinization and fixed in 70 % ethanol. After extensive washing, cells were stained with anti-phospho-histone-H3-Alexa488 (pH3(S10)) antibody (New England Biolabs, Frankfurt, Germany) and PI/RNase staining solution (BD Biosciences, Heidelberg, Germany). Data of 10,000 cells were recorded on an LSRII flow cytometer (BD Biosciences), and cell cycle analyses were performed by using FlowJo 7.6.5 software (Tree Star Inc., Ashland, OR, USA).

Spectral karyotyping (SKY)

Metaphase chromosome spreads were prepared from untreated CAL-33 parental cell line and generated CAL-33 sublines. Colcemid (Roche) was added at a final concentration of 0.1 μg/ml to the culture medium of exponentially growing cells at a density of 6×10^6 cells per 75 cm^2. After 3 h of incubation time, cells were washed with PBS, trypsinized, suspended in fresh culture medium followed by hypotonic KCl treatment (75 mM) at 37 °C for 25 - minutes. Following centrifugation, cells were resuspended in 2–3 ml of fixation solution and approximately 40–50 μl of cell suspension was dropped on several microscope slides. After one week of ageing at room temperature, spectral karyotyping was performed as described by Hieber et al. [14]. The karyotype of each cell line was determined based on a minimum of 15 metaphases. Chromosomal aberrations were detectable by color junctions within affected chromosomes. Spectral imaging and image analysis were performed with a SpectraCube system and SkyView imaging software (both from Applied Spectral Imaging).

Genomic copy number typing (array CGH)

In order to characterize copy number changes of parental CAL-33 and generated CAL-33 sublines, array comparative genomic hybridization analysis (array CGH) was performed on high-resolution oligonucleotide-based SurePrint G3 Human 180 k CGH microarrays (AMADID 252206, Agilent Technologies). DNA from non-irradiated samples was isolated using the QIAamp DNA Mini Kit (Qiagen). The DNA concentration was quantified with the NanoDrop 1000 Spectrophotometer (Thermo Fisher Scientific, Germany). Slight modifications of the original Agilent array CGH protocol were introduced. 250 ng isolated cell line DNA and 250 ng sex-mismatched normal reference DNA (Promega) were labeled with Cy3 and Cy5, respectively, using the CGH labeling kit for oligo arrays (Enzo) following the Enzo's protocol. Microcon YM-30 columns (Millipore) were used to remove the unincorporated nucleotides. Subsequent labeled DNA hybridization, washing and scanning of the CGH arrays were continued according to the Agilent's protocol. The fluorescence intensities were extracted as text files with the Feature Extraction software 10.7 (Agilent Technologies). Obtained data were imported into the R statistical platform (version 3.2.2, www.r-project.org) and filtered for quality outliers using the QA measurements generated by the Feature Extraction software. Experimental artifacts were removed from the array CGH data using spatial normalization as suggested and described in MANOR R-package manual [15] and [16]. Array CGH profiles containing a wave bias that appear as waves in plots were removed using ridge regression based algorithms implemented in NoWaves R-package available from http://www.few.vu.nl/~mavdwiel/nowaves.html [17]. Following normalization and/or wave bias removal, data were segmented using circular binary segmentation algorithms as implemented in DNAcopy R-package [18] in order to detect breakpoints and levels in single array CGH profiles [19]. Chromosomal gains and losses were determined using CGHcall algorithm implemented in CGHcall R-package [20]. To reduce

data complexity, copy number calls were transformed into regions using the R-package CGHregions [21].

Irradiation and sample preparation

Cells were seeded into 6-well plates and allowed to adhere for 16 h. The numbers of plated cells were adjusted to the incubation times: For samples collected 0.25, 2, 7, 12, and 24 h after irradiation, 3.5×10^5 cells/well were seeded, whereas for those collected after 48, 72, and 96 h, 1.75×10^5 cells/well were used. Cells were irradiated at 0 or 8 Gy of gamma-irradiation (Mueller RT-250, Thoraeus Filter, 200 kV, 10 mA) at a dose rate of 1.3 Gy/min, and samples were collected after 0.25, 2, 7, 12, 24, 48, 72, and 96 h by scraping on ice. The washed, dry cell pellet was snap frozen and stored at −80 °C. Samples from 3 independent experiments were used for subsequent transcriptomic analyses. Total RNA was isolated using the Rneasy Mini Kit (Qiagen) including a DNase digestion step, according to the manufacturer's protocol. The concentration of RNA was quantified with a Qubit 2.0 Fluorometer (Life Technologies), and RNA integrity was confirmed with a Bioanalyzer 2100 (Agilent Technologies). Samples with RNA integrity number (RIN) >7 were used in subsequent gene expression microarrays analyses.

Global gene expression profiling

Global gene expression profiling of all CAL-33 cell lines was performed on SurePrint G3 Human Gene Expression 8x60k microarrays (Agilent Technologies, AMADID 28004) using 60 ng of total RNA according to the manufacturer's protocol (one-color Low Input Quick Amp Labeling Kit, Agilent Technologies). Raw gene expression data were extracted as text files with the Feature Extraction software 11.0.1.1 (Agilent Technologies). All data analysis was conducted using the R statistical platform (version 3.2.2, www.r-project.org) [22]. Data quality assessment, filtering, preprocessing, normalization, batch correction based on nucleic acid labeling batches and data analyses were carried out with the Bioconductor R-packages limma, Agi4x44PreProcess and the ComBat function of the sva R-package [23–25]. All quality control, filtering, preprocessing and normalization thresholds were set to the same values as suggested in Agi4x44PreProcess R-package user guide [25]. Only HGNC annotated genes were used in the analysis. For multiple microarray probes representing the same gene the optimal probe was selected according to the Megablast score of probe sequences against the human reference sequence (http://www.ncbi.nlm.nih.gov/refseq/) [26]. If the resulted score was equal for two or more probes, the probe with the lowest differential gene expression FDR value was kept for further analyses since only one expression value per gene was allowed in subsequent gene association network (GAN) reconstruction analysis.

Differential gene expression analysis

The time-course differential gene expression analyses were conducted between irradiated and control cells (sham-irradiated) using a natural cubic spline regression model with three degrees of freedom as described in splineTimeR R-package [27]. Obtained p-values were adjusted by the Benjamini-Hochberg method for false discovery [28]. Genes with an adjusted p-value (FDR, false discovery rate) lower than 0.05 were considered as differentially expressed and associated with radiation response. For the status quo experiment that compares the derived CAL-33 clones with the parental CAL-33 cell line, genes were considered as differentially expressed when a log2 fold-change was higher than 0.5 and a FDR value lower than 0.05.

Identification of early and late responding genes

Temporally differentially expressed genes with fold-change above 2.0 or below 0.5 in any measured time points within the first day after irradiation were considered as early responding genes. Respectively, genes with fold-change above 2.0 or below 0.5 within the second, third or fourth day of irradiation were considered as late responding.

Gene association network reconstruction and identification of important nodes in the reconstructed networks

Temporally differentially expressed genes were subjected to gene association network (GAN) reconstruction using a regularized dynamic partial correlation method [29]. Pairwise relationships between genes over time were inferred based on a dynamic Bayesian network model with shrinkage estimation of covariance matrices as implemented in the GeneNet R-package [30]. Analyses were conducted with a posterior probability of 0.95 for each potential undirected edge. Further, in order to determine the importance of each node in the reconstructed association networks, graph topological analyses based on centrality measures were applied [31]. Three most commonly used centrality measures: degree, shortest path betweenness and closeness describing the importance of gene in a network were combined into one centrality measure [32]. For each gene the three centrality values where ranked and the consensus centrality measure for each node was defined as the mean of the three independent centrality ranks.

Pathway enrichment analysis

The Reactome pathway database was used to conduct the pathway enrichment analysis in order to further investigate the functions of the selected sets of differentially expressed genes [33]. Only pathways containing not more than 600 genes and not less than 20 genes were considered. Thereby, too general and too specific pathways

were excluded from the analysis. Statistical significance of enriched pathways was determined by one-sided Fisher's exact test. The resulting p-values were adjusted for FDR using the Benjamini-Hochberg method.

qRT-PCR technical validation of gene expression data

For technical validation of the gene expression microarray data, RNA samples (500 ng) were reversely transcribed using the QuantiTect Reverse Transcription Kit (Qiagen) according to the manufacturer's protocol and subjected to qRT-PCR reactions (10 μl) on a ViiA 7 qPCR system (Life Technologies). The following Taqman® Assays were used (Life Technologies): AKT3 (Hs00987350_m1), GADD45A (Hs01077132_m1), MAL (Hs00360838_m1), HOPX (Hs04188695_m1), HYAL3 (Hs00185910_m1), TUBGCP3 (Hs00902139_m1), RGS16 (Hs00892674_m1), TNFAIP3 (Hs00234713_m1). ACTB (Hs01060665_g1) and GAPDH (Hs99999905_m1) served as endogenous reference genes. Relative expression levels were calculated using the ΔΔCt method and Spearman correlation analyses with microarray data were performed. Validation was considered successful for Spearman's rho > 0.5. Additionally, the fold-change values obtained from microarrays and qRT-PCR were compared.

Results and discussion

Tumor relapse after radiochemotherapy in HNSCC is often linked to intrinsic and/or acquired radioresistance of tumor cells. However, the underlying molecular mechanisms remain largely unknown [9]. To gain knowledge on this fundamental and clinically relevant process, we established an in vitro model of acquired phenotypes of discrepant radiosensitivity in CAL-33 cells. The underlying molecular mechanisms were investigated by static and dynamic global mRNA expression analyses with subsequent network reconstruction and pathway enrichment analyses.

CAL-33 subclones with different phenotypes of radiosensitivity and cytogenetic characteristics

The parental cell line CAL-33 was repeatedly irradiated in order to generate subclones with different phenotypes of radiosensitivity. To analyze acquired alterations in radiosensitivity of the derived CAL-33 subclones, long-term survival upon gamma-irradiation was assessed by colony formation assays (Fig. 1). For further analyses we selected two subclones. Both subclones #303 and #327 showed statistically significant differences (p-values < 0.0001) when compared to the parental CAL-33 cells. Interestingly, subclone #303 showed increased radiosensitivity (sensitive

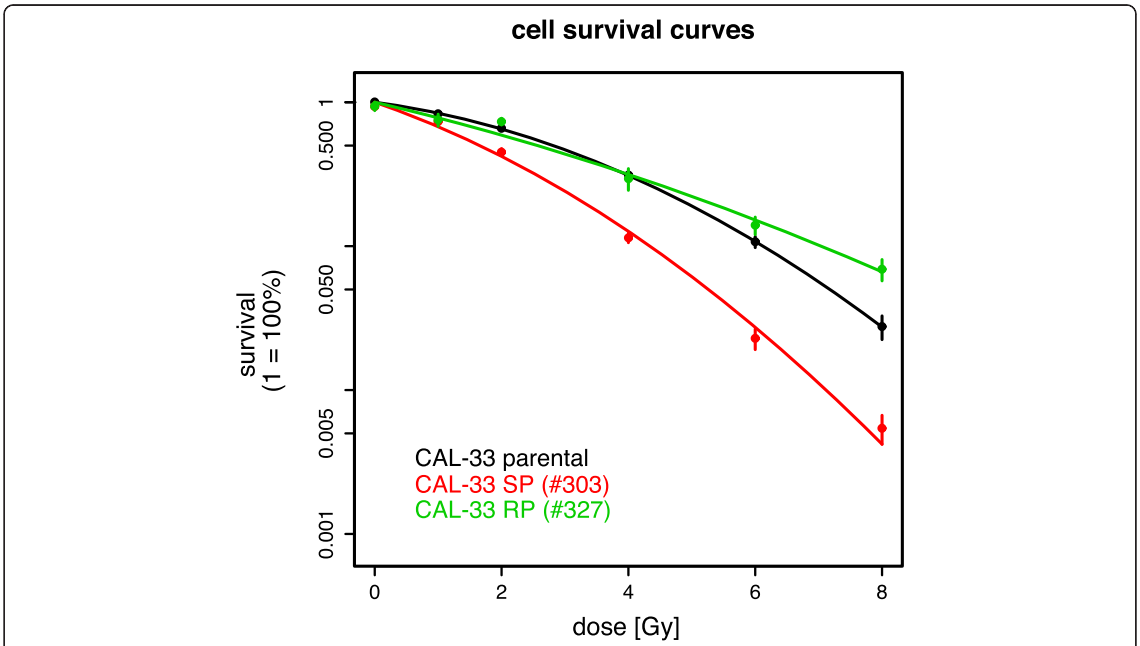

Fig. 1 Dose-survival curves of parental CAL-33 cell line and derived subclones. The linear-quadratic cell survival curves were fitted to the measured data using maximum-likelihood method. Both subclones (SP and RP) showed statistically significant difference (p-values < 0.0001) in response to ionizing radiation compared to the parental CAL-33 cell line

phenotype, SP), whereas subclone #327 was more radioresistant (resistant phenotype, RP) – particularly in the dose range > 4 Gy.

At first glance, the emergence of more radiation sensitive subclones appears unexpected and might be related to clonal evolution that was initiated by the irradiation-induced genomic alterations and that might occur at sublethal doses. This phenomenon has also been observed in previous studies [34, 35]. In comparison to other HNSCC cell lines, CAL-33 is very radioresistant a priori and this might explain why it appears to be very difficult to generate subclones with an even more resistant phenotype.

To analyze structural and numerical chromosomal aberrations in comparison to the parental cell line, the subclones were cytogenetically characterized by SKY analyses. Structural and numerical aberrations identified by SKY in the parental CAL-33 cell line involved chromosomes 3, 7, 8, 9, 16, 18, 20, X, and Y (Fig. 2a). Structural and numerical aberrations of the SP subclone included chromosomes 2, 3, 7, 8, 9, 11, 16, 18, 20, 21, X, and Y (Fig. 2b). Chromosomes 1, 3, 4, 5, 7, 8, 9, 14, 16, 18, 20, X, and Y were affected by aberrations in subclone RP (Fig. 2c).

The obtained SKY results were complemented with copy number analysis by array CGH (Fig. 3 and Additional file 1: Table S1). Array CGH analysis identified 173 regions with aberrant copy number status from which 78, 111 and 132 regions were affected by DNA gains or DNA losses in the CAL-33 parental cells, SP, or RP subclones, respectively (Fig. 3 and Additional file 1: Table S1 and Additional file 2: Table S2). 68 copy number alterations (for SP) and 85 copy number alterations (for RP) were different from the parental CAL-33 cell line. Cytogenetic studies of both clones showed distinct genomic changes in comparison to the parental cell line indicating genomic key alterations for irradiation-related phenotypes on chromosomes 1, 2, 3, 4, 5, 8, 11, 14, 16 and 21. In addition, recurrent CAL-33-specific alterations on chromosomes 3, 7, 18, X and Y were observed showing the authenticity of the newly generated cell lines.

Analysis of proliferation rates and cell cycle distribution

Proliferation rate and cell cycle distribution are important factors, which can affect radiosensitivity and/or resistance. Accordingly, we performed proliferation and cell cycle analyses. In comparison to CAL-33 parental cells, both subclones displayed prolonged doubling times (29 h for subclone SP, 30 h for subclone RP, and 24 h for the parental cell line, Additional file 3: Figure S1, A). This might be due to the observation that under exponential growth conditions, the percentage of mitotic cells in both subclones was decreased (2.1 % for subclone SP, 1.5 % for subclone RP, and 2.9 % for the parental cells), but fails to explain the differences in radiosensitivity (Additional file 3: Figure S1, B). With regard to irradiation-induced G2-arrest, the sensitive subclone SP revealed virtually identical dynamics as the parental CAL-33 cells, whereas in the resistant subclone RP G2-arrest was initially delayed, but also reached its maximum around 12 h after irradiation, and afterwards appeared to be prolonged (Additional file 3: Figure S1, C). In fact, prolonged cell cycle arrest can contribute to radioresistance as cells have more time to repair irradiation-induced DNA damage. However, extended cell cycle arrest can also be indicative for delayed DNA repair. In order to address the mechanisms underlying radioresistance on a molecular level, next we therefore performed unbiased transcriptome analyses of the CAL-33 subclones.

mRNA gene expression analysis of the CAL-33 subclones

Microarray analyses allowed the identification of differences in basal gene expression levels between the derived subclones and the parental CAL-33 cell line. We identified 523 and 1292 differentially expressed genes (FDR < 0.05) for clones SP and RP, respectively, whereas 361 of the genes were overlapping (Additional file 4: Table S3). It is interesting to note that the RP clone exhibited more pronounced transcriptional differences than the SP clone.

Eight of the differentially expressed genes (SP and/or RP clone versus the parental CAL-33 cell line) were arbitrarily chosen for technical validation of the microarray data. Correlation analysis between qRT-PCR and microarray data showed a strong correlation for seven out of eight validated genes (Additional file 5: Table S4). The microarray and qRT-PCR derived fold-changes were in a good agreement.

Subsequently, the differentially expressed genes were subjected to pathway enrichment analyses in order to determine pathways common or specific to the radioresistant or radiosensitive phenotype. In total, 65 and 455 pathways were significantly enriched (FDR < 0.1) for the SP and RP clone, respectively (Additional file 6: Table S5). The top 100 identified pathways ordered according to the highest matching (percentage of differentially expressed genes of all genes in a pathway) were grouped into major pathways (Table 1).

This resulted in a set of commonly deregulated pathways compared to the parental cell line but not specific for a particular phenotype of radiation sensitivity. Moreover, pathways specific to the radiosensitive or radioresistant phenotype were identified. These comprised mainly pathways that are known to be affected by ionizing irradiation in HNSCC [36–38].

Integration of copy number changes with differentially expressed genes

To verify whether the aberrant expression of genes in the SP and RP subclones can be explained by the observed copy number changes, integration of genomic (array CGH data) and transcriptomic data was performed. For subclone

Fig. 2 SKY results of the CAL-33 cell lines. The yellow arrows point the common for all CAL-33 cell lines marker chromosomes. The additional chromosomal rearrangements in analyzed clones compared to the parental CAL-33 cells are marked with white arrows. Structural and numerical aberrations in the parental CAL-33 cell line (**a**) involve chromosomes 3, 7, 8, 9 16, 18, 20, X, and Y. Aberrations of subclone SP (**b**) include chromosomes 2, 3, 7, 8, 9, 11, 16, 18, 20, 21, X, and Y. Chromosomal aberrations of subclone RP (**c**) affect chromosomes 1, 3, 4, 5, 7, 8, 9, 14, 16, 18, 20, X, and Y

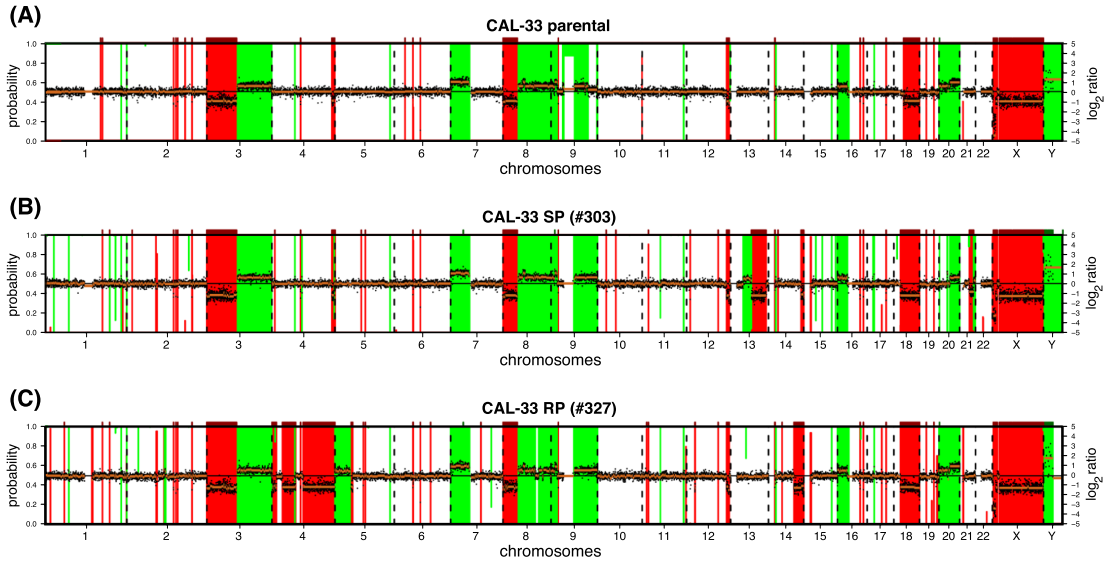

Fig. 3 Array CGH profiles of the CAL-33 cell lines. The array CGH profiles of all of the three cell lines show copy number alterations on several chromosomes: (**a**) parental CAL-33 cell line, (**b**) subclone SP, (**c**) subclone RP. The green bars (starting from the top) represent DNA copy number gains at the corresponding position in the genome, whereas the red bars (starting from the bottom) indicate DNA copy number losses. Bars reaching beyond the middle axis (probability >0.5) were called as gains or losses

SP, we identified 18 genes with DNA gains being up-regulated and 31 genes with DNA losses being down-regulated, whereas for subclone RP, 44 up-regulated genes showed copy number gains and 5 genes with copy number losses were down-regulated (Table 2).

This integrative data analysis of DNA copy number and gene expression followed by pathway enrichment analysis allowed us to identify related pathways encompassing signaling by Rho GTPases as one of the deregulated pathways in the SP subclone. At the same time we observed DNA loss and downregulation of the TIAM1 gene that belongs to the Rho GTPases signaling pathway. Yang et al. recently showed that high expression of TIAM1 is associated with poor clinical outcome in patients with HNSCC [39]. Similarly, for the RP subclone a gain and upregulation of RAD1 and RICTOR genes was observed which is in accordance with the deregulation of the homologous recombination and PI3K signaling pathways in

Table 1 Significantly enriched pathways of genes differentially expressed in subclones SP and RP compared to the parental CAL-33 cells

CAL-33 SP vs parental	Common signalling pathways	CAL-33 RP vs parental
Transmembrane transport of small molecules	Signaling by VEGF	Nonhomologous end-joining (NHEJ)
GPCR ligand binding	Extracellular matrix organization	Homologous DNA pairing and strand exchange
Signaling by Rho GTPases	RNA polymerase III transcription initiation	CD28 dependent PI3K/Akt signaling
	Interferon signaling	NOTCH1 intracellular domain regulates transcription
	Signaling by interleukins	
	Senescence-associated secretory phenotype (SASP)	
	NOD1/2 signaling pathway	
	TNFR1-induced NFkB signaling pathway	
	Toll-like receptors cascades	
	Death receptor signaling	
	MAPK1/MAPK3 signaling	

Pathways common (middle) and specific to the radiosensitive (left) or radioresistant (right) phenotype are shown. The corresponding genes and their direction of regulation (up/down) are listed in Additional file 4: Table S3 and Additional file 6: Table S5

Table 2 Integration of differentially expressed genes with array CGH data

CAL-33 SP (#303)			CAL-33 RP (#327)		
Gene name	FC		Gene name	FC	
PTGS1	16.417	gain	PTGS1	20.52	gain
TLR4	10.333		IL7R	10.643	
SLC2A6	7.167		SLC2A6	7.13	
TNC	5.478		SLC12A7	6.931	
PHF11	4.886		COL5A1	6.608	
PAPPA	4.594		CERCAM	6.381	
MX2	4.457		PDZD2	5.726	
LHFP	4.442		PTGER4	5.05	
RGCC	4.285		STXBP1	4.377	
GTF2F2	3.767		INPP5E	3.797	
BACE2	3.755		NKD2	3.785	
NEK3	3.564		SLC1A3	3.784	
MSANTD3	3.198		RICTOR	3.675	
FNDC3A	2.971		PTGES	3.409	
RC3H2	2.77		MVB12B	3.381	
INPP5E	2.584		CDK5RAP2	3.362	
RPL7A	2.543		PRRC2B	3.155	
UFM1	2.485		SEC16A	2.948	
SLC25A29	0.263	loss	RC3H2	2.855	
RCOR1	0.297		USP20	2.714	
HLCS	0.305		RPL7A	2.59	
CCDC85C	0.318		CARD9	2.572	
IPO5	0.322		TOR1B	2.529	
WRB	0.326		TRAF1	2.524	
PIGP	0.329		QSOX2	2.492	
CDCA4	0.36		TLR4	2.473	
ZBTB42	0.361		UGCG	2.463	
EVA1C	0.37		ZBTB43	2.396	
BTBD6	0.37		C9orf9	2.327	
TTC3	0.374		RAD1	2.255	
CLN5	0.388		TRIM32	2.241	
CCNK	0.389		PTRH1	2.221	
DSC3	0.389		CEP72	2.208	
PPP1R13B	0.389		DAP	2.035	
DYRK1A	0.393		C9orf114	2.019	
SIVA1	0.4		SDHA	2.013	
BRF1	0.404		DOLPP1	1.997	
IMPACT	0.41		RALGPS1	1.996	
IFNGR2	0.416		SURF1	1.958	
TIAM1	0.423		MTRR	1.855	
PCCA	0.426		C5orf42	1.849	
EML1	0.432		ANKRD33B	0.609	
HMGN1	0.439		OR4C6	0.576	
SETD3	0.441		NPR3	0.43	
OSBPL1A	0.462		GOLGA6L6	0.505	loss
IFNAR2	0.54		ZNF480	0.532	
LAMA3	2.1		NBPF10	1.909	
CRIP1	2.463		TPTE	2.342	
CDH2	5.373		NBPF9	2.945	

Detailed information on identified genes, their CNA status and corresponding fold changes are presented

HNSCC as previously described in [40]. For both of those clones a gain and upregulation of the TLR4 gene and the deregulation of the toll-like kinases signaling pathway including upregulation of the genes PLCG2, TAB3, RPS6KA2 has been detected. Even though contradictory reports exist, the overexpression of TLR4 and activation of related pathway has been described to promote HNSCC tumor development and to ensure tumor protection from the immune system [41].

Time-dependent gene expression in response to ionizing radiation in CAL-33 clones

It was hypothesized that CAL-33 subclones with different phenotypes of radiosensitivity also show differences in gene expression profiles in response to irradiation. Therefore, we performed differential time-course microarray analyses between irradiated (8 Gy) and sham irradiated control cells. 7299, 6980, and 8111 genes were differentially expressed in the CAL-33 parental, SP, and RP subclones, respectively (Table 3). Although the number of differentially expressed genes after irradiation with 8 Gy was comparable for all cell lines studied, approximately 50 % of the affected genes were not identical. More than 1000 genes were exclusively involved in the radiation response of each of the CAL-33 cell clones (Fig. 4). The entirety of differentially expressed genes in response to ionizing radiation is listed and compared for all CAL-33 cell lines in Additional file 7: Table S6.

To identify common and separate pathways of the radiation response, pathway enrichment analyses were

Table 3 Comparison of detected and differentially expressed genes after irradiation for analyzed cell sublines

CAL-33 (8 Gy vs sham-irradiated)	Parental cell line	Subclone SP	Subclone RP
Total number of detected genes	12529	12259	12714
Number of differentially expressed genes	7299	6980	8111
Number of genes in the network	6256	5709	6859
5 % top genes	313	285	343

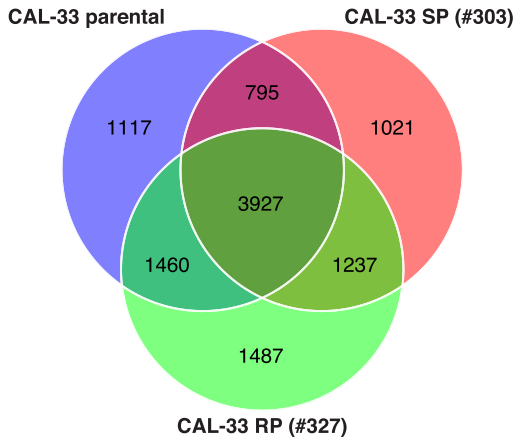

Fig. 4 Venn diagram displaying commonly and exclusively differentially expressed genes of each CAL-33 cell line after irradiation with 8 Gy

Table 4 Significantly enriched pathways of early and late responding genes after ionizing radiation

	Subclone SP	CAL-33 parental	Subclone RP
Early and late responding pathways	Apoptosis		
	Cellular senescence		
	Cell cycle		
	Cellular responses to stress		
	Signaling by Wnt		
	Signaling by Rho GTPases		
Early responding pathways	DNA double-strand break repair		
	Signaling by TGF-beta receptor complex	Interferon signaling	Cellular response to hypoxia
	TRAF6 mediated NF-kB activation		
Late responding pathways	Signaling by TGF-beta receptor complex		
	TRAF6 mediated NF-kB activation		
	Interferon signaling		
	Toll-Like receptors cascades		
	Signaling by interleukins		
	Extracellular matrix organization		
	MAPK family signaling cascades		
	NOD1/2 signaling pathway		
	PI3K/AKT signaling in cancer		
	Signaling by VEGF		
	Signaling by EGFR		
	Signaling by FGFR		
	Signaling by NOTCH		
	Signaling by ERBB2		
	Signaling by ERBB4		
	GPCR ligand binding	Base excision repair	GPCR ligand binding

performed on early and late responding genes, respectively (Additional file 8: Table S7). The most interesting pathways with regard to their known role in radiation response were grouped in to major pathways (Table 4).

It is interesting to note that all cell lines share a set of deregulated pathways (Table 4). In addition, for each of the radiosensitivity phenotypes (parental, SP, RP) specific pathways were observed. The early responses in gene expression include interferon signaling and in particular for the resistant phenotype the cellular response to hypoxia which is known for a long time to have a crucial role in radioresistance [42, 43]. Also, some other pathways from an early gene expression response that are involved in DNA repair, cell cycle, cellular response to stress and apoptosis impact on survival after irradiation and therefore contribute to radioresistance [9, 44–46].

Deregulated pathways related to late responding genes include EGFR- and PI3K/AKT signaling that were already linked to poor clinical outcome and therapy response in HNSCC [47–49] in association with ERBB2, ERBB3 and ERBB4 co-expression [50–52]. Interestingly, also involvement of ERBB2 and EERB4 receptor signaling was observed in all cell lines as a late response to ionizing radiation. Further late responding pathways include toll-like receptor cascades, interleukin signaling, NF-kB activation and interferon signaling all of which are frequently detected after treatment with ionizing radiation [53, 54]. However, the role of interleukin signaling and immune response is largely unknown so far. This also applies to cellular senescence and the impact of senescence pathways on radioresistance that were also discovered as late responding pathways in our CAL-33 subclones. Although evidence exists that senescence might be associated with the disruption of the tissue microenvironment leading to the secretion of senescence-associated pro-inflammatory factors and to the development of a pro-oncogenic environment [34] its role in radioresistance in rather unclear so far.

Gene association network reconstruction and network analysis

To go beyond pathway enrichment analyses of differentially expressed genes, gene association networks were reconstructed. Parameters of the obtained networks (provided as igraph R-objects in Additional file 9: File S1) for all three CAL-33 cell lines are presented in Table 3. Subsequently, the combined topological centrality measure was used to characterize the biological importance of genes in the reconstructed association networks. We identified nodes (genes) that are likely to control the network by combining three network centrality measures: degree,

closeness and shortest path betweenness [32, 55]. The 5 % of the highest ranked genes (listed in Additional file 10: Table S8) were mapped to the Reactome pathways to further evaluate their biological roles. The top ten pathways according to the FDR values are listed in Table 5. All identified pathways are listed in Additional file 11: Table S9. Two of the detected pathways, signaling by Rho GTPases and signaling by Wnt, were in common for all three subclones exposed to irradiation (Table 5). However, most of the pathways were different for the individual subclones. For the parental cell line, we additionally detected pathways associated with cellular response to stress, signaling by

Table 5 The top pathways after mapping of 5 % highest ranked genes from the reconstructed gene association networks to the Reactome pathways

	Pathway	Genes
CAL-33 parental	Generic transcription pathway	CCNC, NR4A3, ZNF248, ZNF302, ZNF350, ZNF417, ZNF431, ZNF543, ZNF621, ZNF710, ZNF735
	Cellular responses to stress	BAG4, CDKN2D, DEDD2, GABARAPL2, HSPA1A, MAPK10, RBX1
	Diseases of signal transduction	CBL, CCNC, CTBP2, FOXO4, RBX1, TGFB1
	EPH-ephrin mediated repulsion of cells	CLTCL1, EFNA5, SRC
	Neurotransmitter release cycle	CHAT, SNAP25, STXBP1
	O-linked glycosylation	ADAMTSL5, CFP, ST3GAL3, THBS2
	Signaling by EGFR	CBL, FOXO4, NF1, PAG1, RBX1, SPRY1, SRC
	Signaling by Wnt	CTBP2, DAAM1, FRAT1, RAC2, RBBP5, RBX1, SOX3
	Signaling by Rho GTPases	ABR, CENPA, DAAM1, PKN3, RAC2, RANGAP1, SRC
	Cytochrome P450 - arranged by substrate type	CYP17A1, CYP3A4, CYP4A11
SP subclone	Axon guidance	APH1A, DPYSL3, HSP90AB1, ITGA9, LAMTOR2, NRG1, PLXNA4, PPP2CA, PSPN, RAC1, RDX, RGMB
	Generic transcription pathway	AKT2, LAMTOR2, MED26, TBL1XR1, ZNF302, ZNF394, ZNF431, ZNF561, ZNF680, ZNF691, ZNF750, ZNF774
	Cell cycle	CDKN2D, EP300, MASTL, MAU2, MCM4, NUPL2, PPP2CA, RAD21, RANGAP1, SKA2, SYCP1
	Chromatin organization	ATXN7, EP300, HIST3H2A, KDM4D, KDM5D, SUPT20H, TBL1XR1
	Diseases of signal transduction	AKT2, APH1A, BCR, CTBP2, EP300, NRG1, PPP2CA, TBL1XR1
	Signaling by Wnt	AKT2, CCDC88C, CTBP2, EP300, PLCB1, PPP2CA, RAC1, RNF146
	Semaphorin interactions	DPYSL3, HSP90AB1, PLXNA4, RAC1
	Glycolysis	ALDOC, GCK, PPP2CA
	Regulation of beta-cell development	AKT2, GCK, IAPP
	RHO GTPases activate WASPs and WAVEs	NCKIPSD, RAC1, WAS
RP subclone	Signaling by Rho GTPases	ABR, ACTB, ARHGAP35, ARHGEF7, BCR, HIST1H2BJ, HIST1H2BL, HIST2H2BE, INCENP, ITSN1, NDE1, OBSCN, RHOT1, SRGAP1, WAS
	Cell Cycle	ANAPC11, BLM, CDKN1A, CDKN2D, FZR1, HIST1H2BJ, HIST1H2BL, HIST2H2BE, INCENP, KIF23, MAU2, NDE1, NUP62, POM121, PSMC3IP, TK2, WHSC1
	Senescence-associated secretory phenotype (SASP)	ANAPC11, CDKN1A, CDKN2D, FZR1, HIST1H2BJ, HIST1H2BL, HIST2H2BE
	GPCR ligand binding	CCL19, GPR132, MC1R, MLN, OPN1SW, OPRL1, PTCH2, PTGDR, PTGER1, TAS2R14, TAS2R19, TAS2R45, TBXA2R, WNT10B
	Transcriptional regulation by small RNAs	HIST1H2BJ, HIST1H2BL, HIST2H2BE, NUP62, POM121
	G alpha (12/13) signaling events	ABR, ARHGEF7, ITSN1, OBSCN, TBXA2R
	Post-translational protein modification	ADAMTS19, ARSB, ARSG, BLM, CFP, CNIH1, CNIH2, GALNT10, NUP62, POM121, ST3GAL3
	DNA repair	ACTB, BLM, CHD1L, DTL, ERCC6, HIST1H2BJ, HIST1H2BL, HIST2H2BE, WHSC1
	Signaling by Wnt	HIST1H2BJ, HIST1H2BL, HIST2H2BE, NFATC1, PLCB1, SOX3, TCF7L2, TMED5, WNT10B
	Assembly of the primary cilium	BBS10, CC2D2A, NDE1, NPHP1, PDE6D, TCTEX1D2, TTC30B

EGFR, and cytochrome P450. The most important pathways in the SP subclone were associated with axon guidance, chromatin organization and semaphorin, whereas for the RP subclone the senescence-associated secretory phenotype (SASP) together with GPCR ligand binding were considered as crucial. The co-occurrence of the SASP and GPCR signaling pathways, that are known to be connected [56], indicate that the identification of those pathways might not be accidental and suggest a high importance for the radiation resistant phenotype. In future experiments more HNSCC cell lines should be analyzed.

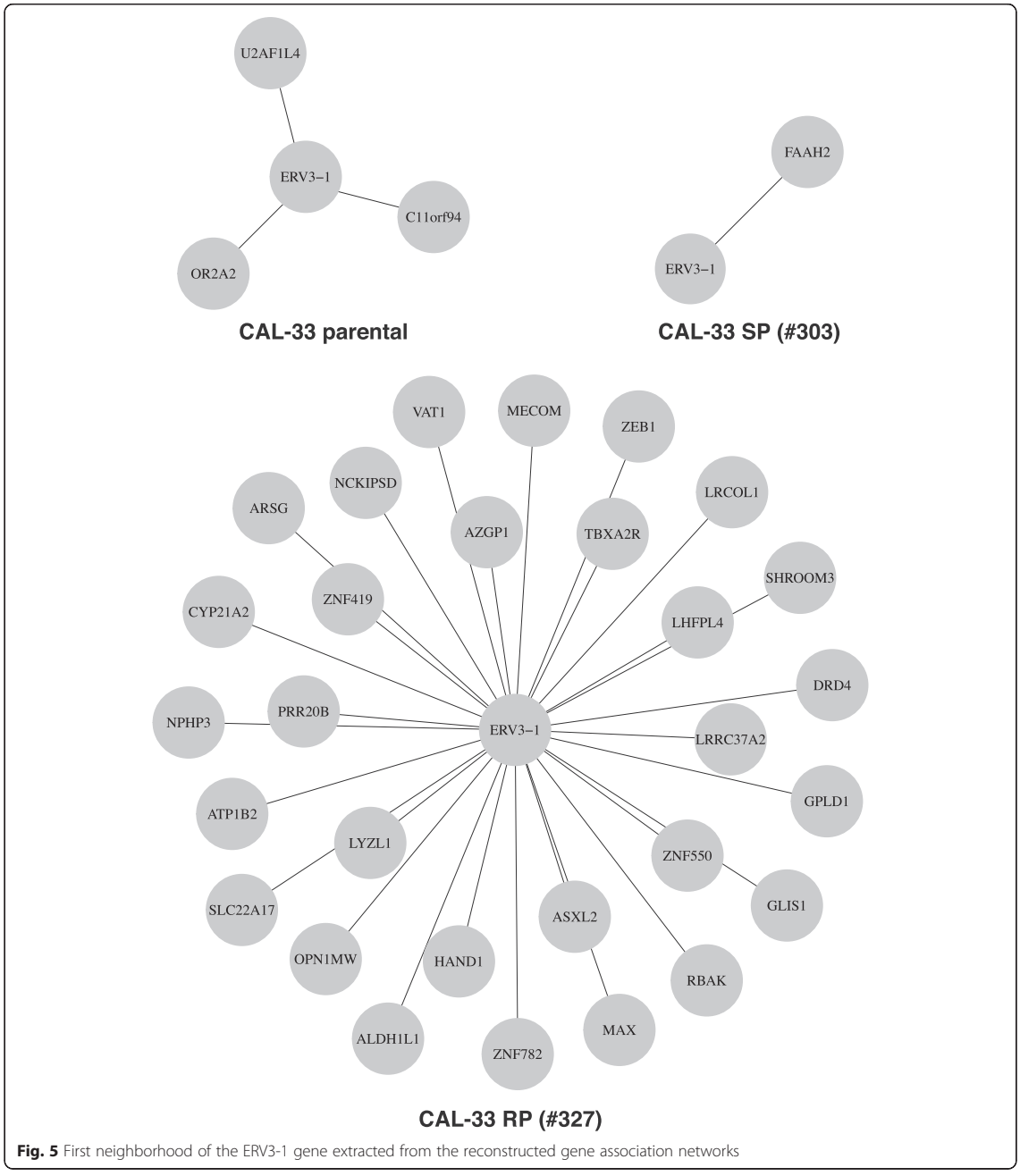

Fig. 5 First neighborhood of the ERV3-1 gene extracted from the reconstructed gene association networks

Expression of endogenous retrovirus and related pathways

The analysis of differentially expressed genes between the RP and SP subclones and the parental cell line revealed the ERVMER34-1 gene as differentially expressed in both clones. Approximately 8 % of the human genome consists of endogenous retroviruses (ERVs) that have been derived from exogenous retroviruses following infection and DNA integration into germ line cells [57, 58]. Although most of the ERV sequences have defective structures, some of ERV genes still have an open reading frame (ORF) and protein expression [59]. ERV genes can promote homologous and non-homologous recombination and therefore, may introduce new mutations [60, 61]. Furthermore, ERVs may lead to genome instability, and contribute to tumor initiation and progression [62]. The expression of ERV genes has been demonstrated in various cancers, including breast, ovarian, prostate and melanoma [63–66]. The differential gene expression analyses of the subclones in comparison to the parental CAL-33 cells revealed ERVMER34-1 gene as differentially expressed in both derived clones (Additional file 4: Table S3). Subsequently, we tested whether any of the retroviral genes were differentially expressed in response to ionizing radiation. Apart from ERVMER34-1, we were able to identify another endogenous retroviral gene, ERV3-1, that was temporally differentially expressed following radiation. The time dependent expression of those genes suggests ERV3-1 expression to be associated with the radiation response, whereas ERVMER34-1 expression exhibits rather random fluctuations (Additional file 12: Figure S2 and Additional file 13: Figure S3). Thus, the ERV3-1 expression clearly implies a possible association with the radiation exposure. The radiation-associated upregulation of ERV3-1 is demonstrated for all subclones starting from the second day of irradiation. To our knowledge, the expression of ERV3-1 following radiation and its influence on radiation resistance has not been addressed in detail so far. A recent study by Lee et al. [67] has demonstrated an increase in the expression of ERV3-1 (HERV-R) *env* related to a fractionated exposure to γ-radiation in radioresistant A549 lung cancer cells but not in less radioresistant H460 cells. The presented results raise the question whether overexpression of ERV3-1 might be involved in the radiation response of HNSCC cells. To gain knowledge about the potential gene interactions with the ERV3-1 gene we used the gene association networks reconstructed for all CAL-33 subclones and extracted the putative direct or indirect ERV3-1 interaction partners resulting in the first neighborhood genes of ERV3-1 differ between the three analyzed cell lines (Fig. 5). The largest first neighborhood gene association network can be observed for the RP subclone where 29 genes are linked to ERV3-1. For the CAL-33 parental cell line and the SP subclone the first neighborhood gene association network consist only of three (OR2A2, U2AF1L4, C11orf94) and one (FEEH2) potential association partners, respectively. The considerably larger first neighborhood of the ERV3-1 gene for the RP cells suggests a more important role of this gene for acquired radiation resistance. In addition, a Reactome pathway enrichment analysis revealed that the first neighborhood genes of the ERV3-1 gene in RP cells were associated with GPCR signaling (DRD4, OPN1MW, TBX A2R), transmembrane transport of small molecules (ATP 1B2, AZGP1, SLC22A17), generic transcription pathway (ZNF419, ZNF550, ZNF782), signaling by Rho GTPases (NCKIPSD), and cell cycle (MAX). However, to our knowledge, the interaction partners of the ERV3-1 gene have not been studied in detail so far, which makes an interpretation difficult and highly speculative at this time. Also further studies have to be performed in order to validate the gene associations with ERV3-1independently.

Conclusion

In conclusion, the present study presents comprehensive gene expression data of CAL-33 subclones of different radiosensitivity. Based on these data networks have been identified that are linked to the radiation response phenotypes. The pathways associated with the resistant phenotype are of special interest focusing on the senescence-associated secretory phenotype (SASP) together and GPCR ligand binding. Also, the radiation-associated expression of the endogenous retrovirus ERV3-1 appears highly attractive for further studies on the molecular mechanisms of acquired radioresistance.

Additional files

Additional file 1: Table S1. Regions of copy number changes identified by array CGH analysis. Array CGH analysis identified 173 regions with copy number changed. 78, 111 and 132 regions were identified as gains or losses for the parental cell line, the SP and RP subclones, respectively. Regions with normal copy number status are labeled with "0", DNA-gains are marked with "1" and DNA-losses with "-1". Regions with different copy number variations between clones SP and RP and the parental cell line are marked as "diff". (XLSX 56 kb)

Additional file 2: Table S2. Overview on the cytogenetic aberrations in CAL-33 cells. Clonal structural and numerical chromosomal aberrations detected by SKY and copy number changes detected by array CGH are listed. (DOCX 94 kb)

Additional file 3: Figure S1. Analyses of proliferation rates and cell cycle distribution. Proliferation curves of the CAL-33 parental cell line and the subclones SP and RP are shown in panel (A). Doubling times were determined in the exponential growth phase by semi-log regression. Cell cycle analyses were performed under exponential growth conditions (B). The dynamics of G2-arrest upon irradiation at 4 Gy are shown in figure panel (C). (PDF 318 kb)

Additional file 4: Table S3. Differentially expressed genes and the corresponding fold-changes. (XLSX 117 kb)

Additional file 5: Table S4. Technical validation of microarray data. Eight of the differentially expressed genes detected with the microarray technology were arbitrarily chosen for technical validation by qRT-PCR. Correlation analysis results (Spearman's rho coefficient) and fold-changes

(microarray and qRT-PCR) are shown. Asterisks (*) indicate fold-change values for genes detected as differentially expressed by microarray analysis. (DOCX 52 kb)

Additional file 6: Table S5. Pathway enrichment analysis results of differentially expressed genes in clones SP and RP in comparison to parental CAL-33 cells. (XLSX 46 kb)

Additional file 7: Table S6. Differentially expressed genes in response to irradiation with 8 Gy for all CAL-33 cell lines. Differentially expressed genes are listed together with the corresponding fold-changes. Additionally, commonly and exclusively differentially expressed genes have been included. (XLSX 2575 kb)

Additional file 8: Table S7. Significantly enriched pathways of early and late responding genes after irradiation with 8 Gy. Pathways with FDR < 0.1 were considered statistically significant. (XLSX 102 kb)

Additional file 9: File S1. Reconstructed gene association networks. All obtained gene association networks are provided as R-objects of type igraph. (RDATA 32863 kb)

Additional file 10: Table S8. 5 % most important genes identified by centrality measures. The 5 % highest ranked genes from the reconstructed gene association networks together with corresponding ranks of centrality measures are shown. (XLSX 88 kb)

Additional file 11: Table S9. Involved pathways after mapping of 5 % highest ranked genes from the gene association networks to the Reactome pathways. The pathways together with the mapped most important (5 % highest ranked) genes are inluded. (XLSX 92 kb)

Additional file 12: Figure S2. Temporal expression and corresponding fold-changes of gene ERVMER34-1 after irradiation with 8 Gy. (PDF 535 kb)

Additional file 13: Figure S3. Temporal expression and corresponding fold-changes of gene ERV3-1 after irradiation with 8 Gy. (PDF 531 kb)

Abbreviations
CGH, comparative genomic hybridization; CNA, copy number aberration; ERV endogenous retrovirus; FDR, false discovery rate; GAN, gene association network; HNSCC, head and neck squamous cell carcinoma; RP, resistant phenotype; SKY, spectral karyotyping; SP, sensitive phenotype

Acknowledgement
We thank Aaron Selmaier, Isabella Zagorski and Laura Dajka from the Research Unit Radiation Cytogenetics for their excellent technical support.

Funding
This study was supported by the German Federal Ministry of Education and Research (ZiSS - 02NUK024B and 02NUK024C) and the Clinical Cooperation Group "Personalized Radiotherapy in Head and Neck Cancer".

Availability of data and material
Gene expression microarray data will be available at ArrayExpress.

Authors' contributions
AM: gene expression analyses, bioinformatics and biostatistics analysis, manuscript draft; US: generation and characterization of subclones, sample preparation for gene expression analyses; MS: bioinformatics and biostatistics analysis; HZ: spectral karyotyping; support for study design, critical revision of the manuscript; KL: conceived generation of subclones; support for experimental design/concept, critical revision of the manuscript; KU: support for study design, experimental design/concept, bioinformatics and biostatistics analysis; JH: array CGH analyses; support for study design, experimental design/concept; draft and critical revision of manuscript; All authors read and approved the final manuscript.

Competing interests
The authors declare that they have no competing interests.

Consent for publication
Not applicable.

Ethics approval and consent to participate
Not applicable.

Disclosures
Not applicable.

Author details
[1]Research Unit Radiation Cytogenetics, Helmholtz Zentrum München, German Research Center for Environmental Health GmbH, 85764 Neuherberg, Germany. [2]Department of Radiotherapy and Radiation Oncology, Ludwig-Maximilians-University, 81377 Munich, Germany. [3]Clinical Cooperation Group "Personalized Radiotherapy in Head and Neck Cancer", Helmholtz Zentrum München, 85764 Neuherberg, Germany.

Received: 14 June 2016 Accepted: 19 July 2016
Published online: 26 July 2016

References
1. Sanderson RJ, Ironside JAD. Squamous cell carcinomas of the head and neck. BMJ. 2002;325(7368):822–7.
2. Network NCC. NCCN Clinical Practice Guidelines in Oncology: head and neck cancers. Version 2. 2013.
3. Hashibe M, Brennan P, Chuang SC, Boccia S, Castellsague X, Chen C, Curado MP, Dal Maso L, Daudt AW, Fabianova E, et al. Interaction between tobacco and alcohol use and the risk of head and neck cancer: pooled analysis in the International Head and Neck Cancer Epidemiology Consortium. Cancer Epidemiol Biomarkers Prev. 2009;8(2):541–50.
4. Guha N, Boffetta P, Wünsch Filho V, Eluf Neto J, Shangina O, Zaridze D, Curado MP, Koifman S, Matos E, Menezes A, et al. Oral health and risk of squamous cell carcinoma of the head and neck and esophagus: results of two multicentric case–control studies. Am J Epidemiol. 2007;66(10):1159–73.
5. Pannone G, Santoro A, Papagerakis S, Lo Muzio L, De Rosa G, Bufo P. The role of human papillomavirus in the pathogenesis of head & neck squamous cell carcinoma: an overview. Infect Agents Cancer. 2011;6:4.
6. Seiwert TY, Salama JK, Vokes EE. The chemoradiation paradigm in head and neck cancer. Nat Clin Pract Oncol. 2007;4(3):156–71.
7. Bar-Ad V, Palmer J, Yang H, Cognetti D, Curry J, Luginbuhl A, Tuluc M, Campling B, Axelrod R. Current management of locally advanced head and neck cancer: the combination of chemotherapy with locoregional treatments. Semin Oncol. 2014;41(6):798–806.
8. Weichselbaum RR, Beckett MA, Schwartz JL, Dritschilo A. Radioresistant tumor cells are present in head and neck carcinomas that recur after radiotherapy. Int J Radiat Oncol Biol Phys. 1988;15(3):575–9.
9. Perri F, Pacelli R, Della Vittoria Scarpati G, Cella L, Giuliano M, Caponigro F, Pepe S: Radioresistance in head and neck squamous cell carcinoma: biological bases and therapeutic implications. Head Neck. 2015;37(5):763–70.
10. Gioanni J, Fischel JL, Lambert JC, Demard F, Mazeau C, Zanghellini E, Ettore F, Formento P, Chauvel P, Lalanne CM, et al. Two new human tumor cell lines derived from squamous cell carcinomas of the tongue: Establishment, characterization and response to cytotoxic treatment. Eur J Cancer Clin Oncol. 1988;24(9):1445–55.
11. Ernst A, Anders H, Kapfhammer H, Orth M, Hennel R, Seidl K, Winssinger N, Belka C, Unkel S, Lauber K. HSP90 inhibition as a means of radiosensitizing resistant, aggressive soft tissue sarcomas. Cancer Lett. 2015;365(2):211–22.
12. Braselmann H, Michna A, Hess J, Unger K. CFAssay: statistical analysis of the colony formation assay. Radiat Oncol. 2015;10:223.
13. Kinzel L, Ernst A, Orth M, Albrecht V, Hennel R, Brix N, Frey B, Gaipl US, Zuchtriegel G, Reichel CA, et al. A novel HSP90 inhibitor with reduced hepatotoxicity synergizes with radiotherapy to induce apoptosis, abrogate clonogenic survival, and improve tumor control in models of colorectal cancer. Oncotarget. 2016. doi:10.18632/oncotarget.9774.
14. Hieber L, Huber R, Bauer V, Schäffner Q, Braselmann H, Thomas G, Bogdanova T, Zitzelsberger H. Chromosomal rearrangements in post-Chernobyl papillary thyroid carcinomas: evaluation by spectral karyotyping and automated interphase FISH. J Biomed Biotechnol. 2011;2011:693691.
15. Neuvial P, Hupe P. MANOR: CGH Micro-Array NORmalization. R package version 1.42.0.
16. Neuvial P, Hupe P, Brito I, Liva S, Manie E, Brennetot C, Radvanyi F, Aurias A, Barillot E. Spatial normalization of array-CGH data. BMC Bioinformatics. 2006;7(264):1–20.
17. van de Wiel MA, Brosens R, Eilers PHC, Kumps C, Meijer GA, Menten B, Sistermans E, Speleman F, Timmerman ME, Ylstra B. Smoothing waves in array CGH tumor profiles. Bioinformatics. 2009;25(9):1099–104.

18. Seshan VE, Olshen A. DNAcopy: DNA copy number data analysis. R package version 1.44.0.
19. Olshen AB, Venkatraman ES, Lucito R, Wigler M. Circular binary segmentation for the analysis of array-based DNA copy number data. Biostatistics. 2004;5(4):557–72.
20. van de Wiel MA, Kim KI, Vosse SJ, van Wieringen WN, Wilting SM, Ylstra B. CGHcall: calling aberrations for array CGH tumor profiles. Bioinformatics. 2007;23(7):892–4.
21. van de Wiel MA, van Wieringen WN. CGHregions: dimension reduction for array CGH data with minimal information loss. Cancer Informatics. 2007;3:55–63.
22. R Core Team: R: A language and environment for statistical computing 2013.
23. Smyth GK. Limma: linear models for microarray data. In: Bioinformatics and Computational Biology Solutions Using {R} and Bioconductor. New York: Springer; 2005. p. 397–420.
24. Gentleman RC, Carey VJ, Bates DM, Bolstad B, Dettling M, Dudoit S, Ellis B, Gautier L, Ge Y, Gentry J, et al. Bioconductor: open software development for computational biology and bioinformatics. Genome Biol. 2004;5(10):R80.
25. Lopez-Romero P: Agi4x44PreProcess: PreProcessing of Agilent 4x44 array data. R package version 1.16.0.
26. Li Q, Birkbak NJ, Gyorffy B, Szallasi Z, Eklund AC. Jetset: selecting the optimal microarray probe set to represent a gene. BMC Bioinformatics. 2011;12:474.
27. Michna A. splineTimeR: Time-course differential gene expression data analysis using spline regression models followed by gene association network reconstruction. R package version 0995 2015.
28. Benjamini Y, Hochberg Y. Controlling the false discovery rate: a practical and powerful approach to multiple testing. J Royal Stat Soc. 1995;57:289–300.
29. Opgen-Rhein R, Strimmer K. Using regularized dynamic correlation to infer gene dependency networks from time-series microarray data. The 4th International Workshop on Computational Systems Biology, WCSB 2006.
30. Opgen-Rhein R, Strimmer K. From correlation to causation networks: a simple approximate learning algorithm and its application to high-dimensional plant gene expression data. BMC Syst Biol. 2007;1:37.
31. Koschützki D, Schreiber F. Centrality analysis methods for biological networks and their application to gene regulatory networks. Gene Regulation Syst Biol. 2008;2:193–201.
32. Abbasi A, Hossain L. Hybrid Centrality Measures for Binary and Weighted Networks. In: Menezes R, Evsukoff A, González MC, editors. Complex Networks. Volume 424, edn. Berlin: Springer; 2013. p. 1–7.
33. Matthews L, Gopinath G, Gillespie M, Caudy M, Croft D, de Bono B, Garapati P, Hemish J, Hermjakob H, Jassal B, et al. Reactome knowledgebase of human biological pathways and processes. Nucleic Acids Res. 2009;37(Database issue):D619–22.
34. Sabin RJ, Anderson RM. Cellular Senescence - its role in cancer and the response to ionizing radiation. Genome Integr. 2011;2(1):7.
35. Wang J, Hu L, Gupta N, Shamseldin T, Ozawa T, Klem J, Cardell M, Deen DF. Induction and characterization of human glioma clones with different radiosensitivities. Neoplasia. 1999;1(2):138–44.
36. Bentzen SM, Atasoy BM, Daley FM, Dische S, Richman PI, Saunders MI, Trott KR, Wilson GD. Epidermal growth factor receptor expression in pretreatment biopsies from head and neck squamous cell carcinoma as a predictive factor for a benefit from accelerated radiation therapy in a randomized controlled trial. J Clin Oncol. 2005;23(24):5560.
37. Kalyankrishna S, Grandis JR. Epidermal growth factor receptor biology in head and neck cancer. J Clin Oncol. 2006;24(17):2666–72.
38. Stadler ME, Patel MR, Couch ME, Hayes DN. Molecular biology of head and neck cancer: risks and pathways. Hematol Oncol Clin North Am. 2008;22(6):1099–124.
39. Yang H, Cai YC, Cao Y, Song M, An X, Xia Y, Wei J, Jiang WQ, Shi YX. The prognostic value of Tiam1 protein expression in head and neck squamous cell carcinoma: a retrospective study. Chin J Cancer. 2015;34(12):614–21.
40. Lui VW, Hedberg ML, Li H, Vangara BS, Pendleton K, Zeng Y, Lu Y, Zhang Q, Du Y, Gilbert BR, et al. Frequent mutation of the PI3K pathway in head and neck cancer defines predictive biomarkers. Cancer Discov. 2013;3(7):761–9.
41. Szczepanski MJ, Czystowska M, Szajnik M, Harasymczuk M, Boyiadzis M, Kruk-Zagajewska A, Szyfter W, Zeromski J, Whiteside TL. Triggering of Toll-like receptor 4 expressed on human head and neck squamous cell carcinoma promotes tumor development and protects the tumor from immune attack. Cancer Res. 2009;69(7):3105–13.
42. Overgaard J. Hypoxic modification of radiotherapy in squamous cell carcinoma of the head and neck - a systematic review and meta-analysis. Radiother Oncol. 2011;100(1):22–32.
43. Li JZ, Gao W, Chan JY, Ho WK, Wong TS. Hypoxia in head and neck squamous cell carcinoma. ISRN Otolaryngol. 2012;2012:708974.
44. Meijer TW, Kaanders JH, Span PN, Bussink J. Targeting hypoxia, HIF-1, and tumor glucose metabolism to improve radiotherapy efficacy. Clin Cancer Res. 2012;18(20):5585–94.
45. Parkin DM, Bray F, Ferlay J, Pisani P. Global cancer statistics, 2002. CA Cancer J Clin. 2005;55(2):74–108.
46. Vokes EE, Weichselbaum RR, Lippman SM, Hong WK. Head and neck cancer. N Engl J Med. 1993;328(3):184–94.
47. Sharafinski ME, Ferris RL, Ferrone S, Grandis JR. Epidermal growth factor receptor targeted therapy of squamous cell carcinoma of the head and neck. Head Neck. 2010;32(10):1412–21.
48. Ang KK, Berkey BA, Tu X, Zhang HZ, Katz R, Hammond EH, Fu KK, Milas L. Impact of epidermal growth factor receptor expression on survival and pattern of relapse in patients with advanced head and neck carcinoma. Cancer Res. 2002;62(24):7350–6.
49. Nijkamp MM, Span PN, Bussink J, Kaanders JH. Interaction of EGFR with the tumour microenvironment: implications for radiation treatment. Radiother Oncol. 2013;108(1):17–23.
50. Ibrahim SO, Vasstrand EN, Liavaag PG, Johannessen AC, Lillehaug JR. Expression of c-erbB proto-oncogene family members in squamous cell carcinoma of the head and neck. Anticancer Res. 1997;17(6D):4539–46.
51. Xia W, Lau YK, Zhang HZ, Liu AR, Li L, Kiyokawa N, Clayman GL, Katz RL, Hung MC. Strong correlation between c-erbB-2 overexpression and overall survival of patients with oral squamous cell carcinoma. Clin Cancer Res. 1997;3(1):3–9.
52. Shintani S, Funayama T, Yoshihama Y, Alcalde RE, Matsumura T. Prognostic significance of ERBB3 overexpression in oral squamous cell carcinoma. Cancer Lett. 1995;95(1–2):79–83.
53. Di Maggio FM, Minafra L, Forte GI, Cammarata FP, Lio D, Messa C, Gilardi MC, Bravatà V. Portrait of inflammatory response to ionizing radiation treatment. J Inflamm (Lond). 2015;12:14.
54. Roses RE, Xu M, Koski GK, Czerniecki BJ. Radiation therapy and Toll-like receptor signaling: implications for the treatment of cancer. Oncogene. 2008;27(2):200–7.
55. Koschützki D. Network Centralities. In: Junker BH, Schreiber F, editors. Analysis of Biological Networks. Hoboken: Wiley; 2007. p. 65–84.
56. Acosta JC, O'Loghlen A, Banito A, Guijarro MV, Augert A, Raguz S, Fumagalli M, Da Costa M, Brown C, Popov N, et al. Chemokine signaling via the CXCR2 receptor reinforces senescence. Cell. 2008;133(6):1006–18.
57. Lander ES, Linton LM, Birren B, Nusbaum C, Zody MC, Baldwin J, Devon K, Dewar K, Doyle M, FitzHugh W, et al. Initial sequencing and analysis of the human genome. Nature. 2001;409(6822):860–921.
58. Löwer R, Löwer J, Kurth R. The viruses in all of us: characteristics and biological significance of human endogenous retrovirus sequences. Proc Natl Acad Sci U S A. 1996;93(11):5177–84.
59. Villesen P, Aagaard L, Wiuf C, Pedersen FS. Identification of endogenous retroviral reading frames in the human genome. Retrovirology. 2004;1:32.
60. Hughes JF, Coffin JM. Evidence for genomic rearrangements mediated by human endogenous retroviruses during primate evolution. Nat Genet. 2001;29(4):487–9.
61. Whitelaw E, Martin DI. Retrotransposons as epigenetic mediators of phenotypic variation in mammals. Nat Genet. 2001;27(4):361–5.
62. Stoye JP. Studies of endogenous retroviruses reveal a continuing evolutionary saga. Nat Rev Microbiol. 2012;10(6):395–406.
63. Wang-Johanning F, Rycaj K, Plummer JB, Li M, Yin B, Frerich K, Garza JG, Shen J, Lin K, Yan P, et al. Immunotherapeutic potential of anti-human endogenous retrovirus-K envelope protein antibodies in targeting breast tumors. J Natl Cancer Inst. 2012;104(3):189–210.
64. Wang-Johanning F, Liu J, Rycaj K, Huang M, Tsai K, Rosen DG, Chen DT, Lu DW, Barnhart KF, Johanning GL. Expression of multiple human endogenous retrovirus surface envelope proteins in ovarian cancer. Int J Cancer. 2007;120(1):81–90.
65. Wang-Johanning F, Frost AR, Jian B, Azerou R, Lu DW, Chen DT, Johanning GL. Detecting the expression of human endogenous retrovirus E envelope transcripts in human prostate adenocarcinoma. Cancer. 2003;98(1):187–97.

66. Li Z, Sheng T, Wan X, Liu T, Wu H, Dong J. Expression of HERV-K correlates with status of MEK-ERK and p16INK4A-CDK4 pathways in melanoma cells. Cancer Invest. 2010;28(10):1031–7.
67. Lee JR, Jung YD, Kim YH, Park SJ, Huh JW, Kim HS. Effects of HERV-R env knockdown in combination with ionizing radiation on apoptosis-related gene expression in A549 lung cancer cells. Biochem Physiol. 2016;5:1.

Conclusion and outlook

The aim of this cumulative thesis was the establishment of a biostatistical method for the analysis of longitudinal gene expression data and the application of this method for the identification of signaling pathways involved in the radiation responses of 1) normal lymphoblastoid cells differing in their radiation sensitivity and 2) tumor HNSCC cells differing in their radiation resistance.

Several different algorithms have been suggested to analyze time-course transcriptomic data with regard to differential expression between treatment groups [121–124]. However, all those methods suffer from different limitations from which the need for relatively high number of measured data points and the demand for inclusion of biological and/or technical replicates are the most disadvantageous. The natural cubic spline regression method for the detection of temporally differentially expressed genes presented within this thesis does not require any replicates and additionally allows for the adaptation of the applied spline models depending on the number of collected data points. Moreover, the proposed algorithm does not need identical sampling times for the compared treatments groups, which for the majority of methods is compulsory. The introduced method can be applied also on incomplete time-course data sets, what is especially important for studies with limited sample source where for technical reasons some samples had to be excluded and cannot be repeatedly generated. Therefore, the method is useful and applicable also to data that were not particularly generated for time-course gene expression studies including already existing data sets from clinical samples. Re-analysis of previously generated time-course data often allows to address new clinical questions and find new important values to the existing data.

To ensure the access of the proposed method for other users and future applications, I have implemented, described and provided the biostatistical approach developed within this thesis as an R software package "splineTimeR" which is freely available via the Bioconductor project at https://www.bioconductor.org [125].

The performance of the approach introduced within this thesis has been compared and validated with another established method for the temporal gene expression data analysis called BETR that has shown the best performance over other commonly used methods [126]. Both compared methods detected the same biological processes as the most important with regard to the radiation response in normal cells as presented in the first publication, thereby proving the plausibility of the spline-based method. However, the spline method was able to detect more differentially expressed genes than the BETR method, which was shown to detect only 65% of truly differentially expressed genes [126]. Therefore, the proposed spline-based method allows achieving higher identification rates of temporally differentially expressed genes.

In the first study (publication I), the application of the spline differential expression method in combination with network reconstruction and pathway enrichment analyses provided insight into the mechanisms that might be relevant for the acute radiation response of normal cells. The obtained results revealed the impact of senescence-associated pathways and raised the question about the influence of senescent cells on radiotherapy outcome. Future experiments using clinical samples have to evaluate the role of senescence in acute radiation response of tumor surrounding normal tissues.

In the second study (publication II), the proposed data analysis workflow has been used to identify pathways that may have an important impact on radioresistance of HNSCC cancer cells. Senescence-associated secretory phenotype (SASP) and GPCR ligand binding were the most important and significantly deregulated signaling pathways identified for the resistant phenotype after exposure to ionizing radiation. The co-occurrence of the SASP and GPCR signaling pathway, that are known to interplay [127], implies that the identification of those pathways might not be coincidental and suggests a high importance for the radiation resistant phenotype. However, this hypothesis has to be validated in subsequent studies with clinical data.

This thesis represents a statistical effort to elucidate the molecular mechanisms of the radiation responses of therapeutically relevant cells. Mathematical modeling of biological or clinical data has a potential to be beneficial in therapy treatment planning. The mathematical models may help to understand the underlying molecular

processes and to predict the success of new treatment strategies. *In silico* modeling of radiation response is emerging as an important tool for treatment simulations, outcome predictions and therapy optimization, which can contribute to the improvement of the therapy treatment. There is a particular need for modeling of the identified pathways from this thesis by perturbation experiments as already exemplified by Klinger et al. for EGFR-related pathways in colon cancer cell lines [87]. Interdisciplinary research leading to predictive models not only of radiation response by implementing biostatistical techniques needs to be encouraged to enable further developments in the clinical diagnostics and sophisticated treatment planning.

Bibliography

[1] Delaney G, Jacob S, Featherstone C, Barton M. The role of radiotherapy in cancer treatment: estimating optimal utilization from a review of evidence-based clinical guidelines. Cancer. 2005;104(6):1129–1137.

[2] Begg AC, Stewart FA, Vens C. Strategies to improve radiotherapy with targeted drugs. Nat Rev Cancer. 2011;11(4):239–253.

[3] Bernier J, Hall EJ, Giaccia A. Radiation oncology: a century of achievements. Nat Rev Cancer. 2004;4(9):737–747.

[4] Withers HR. The four R's of radiotherapy. Adv Radiat Biol. 1975;5:241–247.

[5] Withers HR. Treatment-induced accelerated human tumor growth. Semin Radiat Oncol. 1993;3(2):135–143.

[6] Withers HR, Maciejewski B, Taylor JM, Hliniak A. Accelerated repopulation in head and neck cancer. Front Radiat Ther Oncol. 1988;22:105–110.

[7] Bese NS, Sut PA, Ober A. The effect of treatment interruptions in the postoperative irradiation of breast cancer. Oncology. 2005;69(3):214–223.

[8] Kim JJ, Tannock IF. Repopulation of cancer cells during therapy: an important cause of treatment failure. Nat Rev Cancer. 2005;5(7):516–525.

[9] Bristow RG, Hill RP. Hypoxia and metabolism. Hypoxia, DNA repair and genetic instability. Nat Rev Cancer. 2008;8(3):180–192.

[10] Steel GG, McMillan TJ, Peacock JH. The 5Rs of radiobiology. Int J Radiat Biol. 1989;56(6):1045–1048.

[11] Begg AC. Molecular targeting and patient individualization. In: Basic Clinical Radiobiology. Hodder Arnold, London. 2009;4th edition.

[12] Begg AC. Predicting recurrence after radiotherapy in head and neck cancer. Semin Radiat Oncol. 2012;22(2):108–118.

[13] Sanderson RJ, Ironside JAD. Squamous cell carcinomas of the head and neck. BMJ. 2002;325(7368):822–827.

[14] Network NCC. NCCN Clinical Practice Guidelines in Oncology: head and neck cancers. Version 2. 2013;.

[15] Hashibe M, Brennan P, Chuang SC, Boccia S, Castellsague X, Chen C, et al. Interaction between tobacco and alcohol use and the risk of head and neck cancer: pooled analysis in the International Head and Neck Cancer Epidemiology Consortium. Cancer Epidemiol Biomarkers Prev. 2009;8(2):541–550.

[16] Guha N, Boffetta P, Wünsch Filho V, Eluf Neto J, Shangina O, Zaridze D, et al. Oral health and risk of squamous cell carcinoma of the head and neck and esophagus: results of two multicentric case-control studies. Am J Epidemiol. 2007;66(10):1159–1173.

[17] Pannone G, Santoro A, Papagerakis S, Lo Muzio L, De Rosa G, Bufo P. The role of human papillomavirus in the pathogenesis of head and neck squamous cell carcinoma: an overview. Infect Agent Cancer. 2011;6(6).

[18] Perri F, Pacelli R, Della Vittoria Scarpati G, Cella L, Giuliano M, Caponigro F, et al. Radioresistance in head and neck squamous cell carcinoma: biological bases and therapeutic implications. Head Neck. 2015;37(5):763–770.

[19] Baumann M, Krause M, Overgaard J, Debus J, Bentzen SM, Daartz J, et al. Radiation oncology in the era of precision medicine. Nat Rev Cancer. 2016;16(4):234–249.

[20] Greve B, Bölling T, Amler S, Rössler U, Gomolka M, Mayer C, et al. Evaluation of different biomarkers to predict individual radiosensitivity in an inter-laboratory comparison - lessons for future studies. PLoS One. 2012;7(10):e47185.

[21] Rubin, P, Casarette GW. Clinical radiation pathology. Philadelphia: Saunders. 1968;.

[22] Miller AR, Martenson JA, Nelson H, Schleck CD, Ilstrup DM, Gunderson LL, et al. The incidence and clinical consequences of treatment-related bowel injury. Int J Radiat Oncol Biol Phys. 1999;43(4):817–825.

[23] Turesson I, Nyman J, Holmberg E, Odén A. Prognostic factors for acute and late skin reactions in radiotherapy patients. Int J Radiat Oncol Biol Phys. 1996;36(5):1065–1075.

[24] Weichselbaum RR, Beckett MA, Schwartz JL, Dritschilo A. Radioresistant tumor cells are present in head and neck carcinomas that recur after radiotherapy. Int J Radiat Oncol Biol Phys. 1988;15(3):575–579.

[25] Orth M, Lauber K, Niyazi M, Friedl AA, Li M, Maihoefer C, et al. Current concepts in clinical radiation oncology. Radiat Environ Biophys. 2014;53(1):1–29.

[26] Ang KK, Andratschke NH, Milas L. Epidermal growth factor receptor and response of head-and-neck carcinoma to therapy. Int J Radiat Oncol Biol Phys. 2004;58(3):959–965.

[27] Franken NA, Rodermond HM, Stap J, Haveman J, van Bree C. Clonogenic assay of cells in vitro. Nat Protoc. 2006;1(5):2315–2319.

[28] Munshi A, Hobbs M, Meyn RE. Clonogenic cell survival assay. In: Chemosensitivity. Methods in Molecular Medicine. 2005;.

[29] Williams JR, Zhang Y, Russell J, Koch C, Little JB. Human tumor cells segregate into radiosensitivity groups that associate with ATM and TP53 status. Acta Oncol. 2007;46(5):628–638.

[30] Guertler A, Kraemer A, Roessler U, Hornhardt S, Kulka U, Moertl S, et al. The WST survival assay: an easy and reliable method to screen radiation-sensitive individuals. Radiat Prot Dosimetry. 2011;143(2-4):487–490.

[31] Sachs RK, Chen PL, Hahnfeldt PJ, Hlatky LR. DNA damage caused by ionizing radiation. Math Biosci. 1992;112(2):271–303.

[32] Dianov GL, O'Neill P, Goodhead DT. Securing genome stability by orchestrating DNA repair: removal of radiation-induced clustered lesions in DNA. Bioessays. 2001;23(8):745–749.

[33] Jeggo, P, Lavin MF. Cellular radiosensitivity: how much better do we understand it? Int J Radiat Biol. 2009;85(12):1061–1081.

[34] Boucher D, Testard I, Averbeck D. Low levels of clustered oxidative DNA damage induced at low and high LET irradiation in mammalian cells. Radiat Environ Biophys. 2006;45(4):267–276.

[35] Shiloh Y. ATM and related protein kinases: safeguarding genome integrity. Nat Rev Cancer. 2003;3(3):155–168.

[36] Abraham RT. Cell cycle checkpoint signaling through the ATM and ATR kinases. Genes Dev. 2001;15(17):2177–2196.

[37] Zhang XP, Liu F, Wang W. Two-phase dynamics of p53 in the DNA damage response. Proc Natl Acad Sci U S A. 2011;108(22):8990–8995.

[38] Verheij M. Clinical biomarkers and imaging for radiotherapy-induced cell death. Cancer Metastasis Rev. 2008;27(3):471–480.

[39] Eriksson D, Stigbrand T. Radiation-induced cell death mechanisms. Tumour Biol. 2010;31(4):363–372.

[40] Watters D. Molecular mechanisms of ionizing radiation-induced apoptosis. Immunology and Cell Biology. 1999;77:263–271.

[41] Vakifahmetoglu H, Olsson M, Zhivotovsky B. Death through a tragedy: mitotic catastrophe. Cell Death and Differentiation. 2008;15:1153–1162.

[42] Campisi, J, d'Adda di Fagagna F. Cellular senescence: when bad things happen to good cells. Nat Rev Mol Cell Biol. 2007;8(9):729–740.

[43] Kroemer G, Galluzzi L, Vandenabeele P, Abrams J, Alnemri ES, Baehrecke EH, et al. Classification of cell death: recommendations of the Nomenclature Committee on Cell Death 2009. Cell Death Differ. 2009;16(1):3–11.

[44] Meng Y, Efimova EV, Hamzeh KW, Darga TE, Mauceri HJ, Fu YX, et al. Radiation-inducible immunotherapy for cancer: senescent tumor cells as a cancer vaccine. Mol Ther. 2012;20(5):1046–1055.

[45] Xue W, Zender L, Miething C, Dickins RA, Hernando E, Krizhanovsky V, et al. Senescence and tumour clearance is triggered by p53 restoration in murine liver carcinomas. Nature. 2007;445(7128):656–660.

[46] Kang TW, Yevsa T, Woller N, Hoenicke L, Wuestefeld T, Dauch D, et al. Senescence surveillance of pre-malignant hepatocytes limits liver cancer development. Nature. 2011;479(7374):547–551.

[47] Krtolica A, Parrinello S, Lockett S, Desprez PY, Campisi J. Senescent fibroblasts promote epithelial cell growth and tumorigenesis: a link between cancer and aging.

Proc Natl Acad Sci U S A. 2001;98(21):12072–12077.

[48] Vasile E, Tomita Y, Brown LF, Kocher O, Dvorak HF. Differential expression of thymosin beta-10 by early passage and senescent vascular endothelium is modulated by VPF/VEGF: evidence for senescent endothelial cells in vivo at sites of atherosclerosis. FASEB J. 2001;15(2):458–466.

[49] Price JS, Waters JG, Darrah C, Pennington C, Edwards DR, Donell ST, et al. The role of chondrocyte senescence in osteoarthritis. Aging Cell. 2002;1(1):57–65.

[50] Nelson G, Wordsworth J, Wang C, Jurk D, Lawless C, Martin-Ruiz C, et al. A senescent cell bystander effect: senescence-induced senescence. Aging Cell. 2012;11(2):345–349.

[51] Wu PC, Wang Q, Grobman L, Chu E, Wu DY. Accelerated cellular senescence in solid tumor therapy. Exp Oncol. 2012;34(3):298–305.

[52] Campisi J. Senescent cells, tumor suppression, and organismal aging: good citizens, bad neighbors. Cell. 2005;120(4):513–522.

[53] Dilley TK, Bowden GT, Chen QM. Novel mechanisms of sublethal oxidant toxicity: induction of premature senescence in human fibroblasts confers tumor promoter activity. Exp Cell Res. 2003;290(1):38–48.

[54] Tsai KK, Stuart J, Chuang YY, Little JB, Yuan ZM. Low-dose radiation-induced senescent stromal fibroblasts render nearby breast cancer cells radioresistant. Radiat Res. 2009;172(3):306–313.

[55] Wang Q, Zhu F, Wang Z. Identification of EGF receptor C-terminal sequences 1005-1017 and di-leucine motif 1010LL1011 as essential in EGF receptor endocytosis. Exp Cell Res. 2007;313(15):3349–3363.

[56] Toulany M, Rodemann HP. Membrane receptor signaling and control of DNA repair after exposure to ionizing radiation. Nuklearmedizin. 2010;49 Suppl 1:S26–S30.

[57] Hanada N, Lo HW, Day CP, Pan Y, Nakajima Y, Hung MC. Co-regulation of B-Myb expression by E2F1 and EGF receptor. Mol Carcinog. 2006;45(1):10–17.

[58] Toulany M, Minjgee M, Kehlbach R, Chen J, Baumann M, Rodemann HP. ErbB2 expression through heterodimerization with erbB1 is necessary for ionizing radiation - but not EGF-induced activation of Akt survival pathway. Radiother Oncol. 2010;97(2):338–345.

[59] Dittmann K, Mayer C, Kehlbach R, Rodemann HP. Radiation-induced caveolin-1 associated EGFR internalization is linked with nuclear EGFR transport and activation of DNA-PK. Mol Cancer. 2008;7:69.

[60] Dan HC, Cooper MJ, Cogswell PC, Duncan JA, Ting JP, Baldwin AS. Akt-dependent regulation of NF-kappaB is controlled by mTOR and Raptor in association with IKK. Genes Dev. 2008;22(11):1490–1500.

[61] Paglin S, Lee NY, Nakar C, Fitzgerald M, Plotkin J, Deuel B, et al. Rapamycin-sensitive pathway regulates mitochondrial membrane potential, autophagy, and survival in irradiated MCF-7 cells. Cancer Res. 2005;65(23):11061–70.

[62] Gupta AK, Bakanauskas VJ, Cerniglia GJ, Cheng Y, Bernhard EJ, Muschel RJ, et al. The Ras radiation resistance pathway. Cancer Res. 2001;61(10):4278–4282.

[63] Cengel KA, Voong KR, Chandrasekaran S, Maggiorella L, Brunner TB, Stanbridge E, et al. Oncogenic K-Ras signals through epidermal growth factor receptor and wild-type H-Ras to promote radiation survival in pancreatic and colorectal carcinoma cells. Neoplasia. 2007;9(4):341–348.

[64] Toulany M, Baumann M, Rodemann HP. Stimulated PI3K-AKT signaling mediated through ligand or radiation-induced EGFR depends indirectly, but not directly, on constitutive K-Ras activity. Mol Cancer Res. 2007;5(8):863–872.

[65] Toulany M, Dittmann K, Krueger M, Baumann M, Rodemann HP. Radioresistance of K-Ras mutated human tumor cells is mediated through EGFR-dependent activation of PI3K-AKT pathway. Radiother Oncol. 2005;76(2):143–150.

[66] Stone HB, Moulder JE, Coleman CN, Ang KK, Anscher MS, Barcellos-Hoff MH, et al. Models for evaluating agents intended for the prophylaxis, mitigation and treatment of radiation injuries. Report of an NCI Workshop, December 3-4, 2003. Radiat Res. 2004;162(6):711–728.

[67] Dasari S, Tchounwou PB. Cisplatin in cancer therapy: molecular mechanisms of action. Eur J Pharmacol. 2014;740:364–378.

[68] Ng CE, Bussey AM, Raaphorst GP. Inhibition of potentially lethal and sublethal damage repair by camptothecin and etoposide in human melanoma cell lines. Int J Radiat Biol. 1994;66(1):49–57.

[69] Thorn CF, Oshiro C, Marsh S, Hernandez-Boussard T, McLeod H, Klein TE, et al. Doxorubicin pathways: pharmacodynamics and adverse effects. Pharmacogenet Genomics. 2011;21(7):440–446.

[70] Strese S, Fryknaes M, Larsson R, Gullbo J. Effects of hypoxia on human cancer cell line chemosensitivity. BMC Cancer. 2013;13:331.

[71] Yarbro JW. Mechanism of action of hydroxyurea. Semin Oncol. 1992;19(3 Suppl 9):1–10.

[72] Horwitz SB. Taxol (paclitaxel): mechanisms of action. Ann Oncol. 1994;5 Suppl 6:S3–S6.

[73] Matta A, Ralhan R. Overview of current and future biologically based targeted therapies in head and neck squamous cell carcinoma. Head Neck Oncol. 2009;1:6.

[74] Grandis JR, Tweardy DJ. Elevated levels of transforming growth factor alpha and epidermal growth factor receptor messenger RNA are early markers of carcinogenesis in head and neck cancer. Cancer Res. 1993;53(15):3579–3584.

[75] Bonner JA, Harari PM, Giralt J, Azarnia N, Shin DM, Cohen RB, et al. Radiotherapy plus cetuximab for squamous-cell carcinoma of the head and neck. N Engl J Med. 2006;354(6):567–578.

[76] Bonner JA, Harari PM, Giralt J, Cohen RB, Jones CU, Sur RK, et al. Radiotherapy plus cetuximab for locoregionally advanced head and neck cancer: 5-year survival data from a phase 3 randomised trial, and relation between cetuximab-induced rash

and survival. Lancet Oncol. 2010;11(1):21–28.

[77] Bardelli A, Jänne PA. The road to resistance: EGFR mutation and cetuximab. Nat Med. 2012;18(2):199–200.

[78] Bublil EM, Yarden Y. The EGF receptor family: spearheading a merger of signaling and therapeutics. Curr Opin Cell Biol. 2007;19(2):124–134.

[79] Porter AC, Vaillancourt RR. Tyrosine kinase receptor-activated signal transduction pathways which lead to oncogenesis. Oncogene. 1998;17(11 Reviews):1343–1352.

[80] Bluethgen N, Legewie S. Systems analysis of MAPK signal transduction. Essays Biochem. 2008;45:95–107.

[81] Legewie S, Herzel H, Westerhoff HV, Bluethgen N. Recurrent design patterns in the feedback regulation of the mammalian signalling network. Mol Syst Biol. 2008;4:190.

[82] Cirit M, Wang CC, Haugh JM. Systematic quantification of negative feedback mechanisms in the extracellular signal-regulated kinase (ERK) signaling network. J Biol Chem. 2010;285(47):36736–36744.

[83] Avraham R, Yarden Y. Feedback regulation of EGFR signalling: decision making by early and delayed loops. Nat Rev Mol Cell Biol. 2011;12(2):104–117.

[84] Friday BB, Yu C, Dy GK, Smith PD, Wang L, Thibodeau SN, et al. BRAF V600E disrupts AZD6244-induced abrogation of negative feedback pathways between extracellular signal-regulated kinase and Raf proteins. Cancer Res. 2008;68(15):6145–6153.

[85] Sturm OE, Orton R, Grindlay J, Birtwistle M, Vyshemirsky V, Gilbert D, et al. The mammalian MAPK/ERK pathway exhibits properties of a negative feedback amplifier. Sci Signal. 2010;3(153):ra90.

[86] Fritsche-Guenther R, Witzel F, Sieber A, Herr R, Schmidt N, Braun S, et al. Strong negative feedback from Erk to Raf confers robustness to MAPK signalling. Mol Syst Biol. 2011;7:489.

[87] Klinger B, Sieber A, Fritsche-Guenther R, Witzel F, Berry L, Schumacher D, et al. Network quantification of EGFR signaling unveils potential for targeted combination therapy. Mol Syst Biol. 2013;9(673).

[88] Abdullah-Sayani A, de Mesquita JMB, van de Vijver MJ. Technology insight: tuning into the genetic orchestra using microarrays - limitations of DNA microarrays in clinical practice. Nat Clin Pract Oncol. 2006;3(9):501–516.

[89] Gutman, S, Kessler LG. The US Food and Drug Administration perspective on cancer biomarker development. Nat Rev Cancer. 2006;6(7):565–571.

[90] van't Veer LJ, Dai H, van de Vijver MJ, He YD, Hart AA, Mao M, et al. Gene expression profiling predicts clinical outcome of breast cancer. Nature. 2002;415(6871):530–536.

[91] van de Vijver MJ, He YD, van't Veer LJ, Dai H, Hart AA, Voskuil DW, et al. A gene-expression signature as a predictor of survival in breast cancer. N Engl J Med. 2002;347(25):1999–2009.

[92] Paik S, Shak S, Tang G, Kim C, Baker J, Cronin M, et al. A multigene assay to

predict recurrence of tamoxifen-treated, node-negative breast cancer. N Engl J Med. 2004;351(27):2817–2826.

[93] Wang Y, Klijn JG, Zhang Y, Sieuwerts AM, Look MP, Yang F, et al. Gene-expression profiles to predict distant metastasis of lymph-node-negative primary breast cancer. Lancet. 2005;365(9460):671–679.

[94] Garber ME, Troyanskaya OG, Schluens K, Petersen S, Thaesler Z, Pacyna-Gengelbach M, et al. Diversity of gene expression in adenocarcinoma of the lung. Proc Natl Acad Sci U S A. 2001;98(24):13784–13789.

[95] Beer DG, Kardia SL, Huang CC, Giordano TJ, Levin AM, Misek DE, et al. Gene-expression profiles predict survival of patients with lung adenocarcinoma. Nat Med. 2002;8(8):816–824.

[96] Yeoh EJ, Ross ME, Shurtleff SA, Williams WK, Patel D, Mahfouz R, et al. Classification, subtype discovery, and prediction of outcome in pediatric acute lymphoblastic leukemia by gene expression profiling. Cancer Cell. 2002;1(2):133–143.

[97] Schaner ME, Ross DT, Ciaravino G, Sorlie T, Troyanskaya O, Diehn M, et al. Gene expression patterns in ovarian carcinomas. Mol Biol Cell. 2003;14(11):4376–4386.

[98] Lapointe J, Li C, Higgins JP, van de Rijn M, Bair E, Montgomery K, et al. Gene expression profiling identifies clinically relevant subtypes of prostate cancer. Proc Natl Acad Sci U S A. 2004;101(3):811–816.

[99] Yu YP, Landsittel D, Jing L, Nelson J, Ren B, Liu L, et al. Gene expression alterations in prostate cancer predicting tumor aggression and preceding development of malignancy. J Clin Oncol. 2004;22(14):2790–2799.

[100] Eschrich S, Yang I, Bloom G, Kwong KY, Boulware D, Cantor A, et al. Molecular staging for survival prediction of colorectal cancer patients. J Clin Oncol. 2005;23(15):3526–3535.

[101] Reddy RB, Bhat AR, James BL, Govindan SV, Mathew R, Dr R, et al. Meta-analyses of microarray datasets identifies ANO1 and FADD as prognostic markers of head and neck cancer. PLoS One. 2016;11(1):e0147409.

[102] Viet, CT, Schmidt BL. Understanding oral cancer in the genome era. Head Neck. 2010;32(9):1246–1268.

[103] Ha PK, Chang SS, Glazer CA, Califano JA, Sidransky D. Molecular techniques and genetic alterations in head and neck cancer. Oral Oncol. 2009;45(4-5):335–339.

[104] Alizadeh AA, Eisen MB, Davis RE, Ma C, Lossos IS, Rosenwald A, et al. Distinct types of diffuse large B-cell lymphoma identified by gene expression profiling. Nature. 2000;403(6769):503–511.

[105] Bittner M, Meltzer P, Chen Y, Jiang Y, Seftor E, Hendrix M, et al. Molecular classification of cutaneous malignant melanoma by gene expression profiling. Nature. 2000;406(6795):536–540.

[106] Bumgarner R. Overview of DNA microarrays: types, applications, and their future. Curr Protoc Mol Biol. 2013;Chapter 22:Unit 22.1.

[107] Bar-Joseph Z, Gitter A, Simon I. Studying and modelling dynamic biological processes using time-series gene expression data. Nat Rev Genet. 2012;13(8):552–564.

[108] Oh S, Song S, Grabowski G, Zhao H, Noonan JP. Time series expression analyses using RNA-seq: a statistical approach. Biomed Res Int. 2013;2013:203681.

[109] Bandyopadhyay, S, Bhattacharyya M. A biologically inspired measure for coexpression analysis. IEEE/ACM Trans Comput Biol Bioinform. 2011;8(4):929–942.

[110] Yuan, M, Kendziorski C. Hidden Markov models for microarray time course data in multiple biological conditions. Journal of the American Statistical Association. 2006;101(476):1323–1332.

[111] Gardner TS, di Bernardo D, Lorenz D, Collins JJ. Inferring genetic networks and identifying compound mode of action via expression profiling. Science. 2003;301(5629):102–105.

[112] de Jong H. Modeling and simulation of genetic regulatory systems: a literature review. J Comput Biol. 2002;9(1):67–103.

[113] Karlebach G, Shamir R. Modelling and analysis of gene regulatory networks. Nat Rev Mol Cell Biol. 2008;9(10):770–780.

[114] Barabási AL, Oltvai ZN. Network biology: understanding the cell's functional organization. Nat Rev Genet. 2004;5(2):101–113.

[115] Opgen-Rhein, R, Strimmer K. Using regularized dynamic correlation to infer gene dependency networks from time-series microarray data. The 4th International Workshop on Computational Systems Biology, WCSB. 2006;.

[116] Koschützki D. Network centralities. In: Analysis of Biological Networks. Wiley. 2007;.

[117] Abbasi A, Hossain L. Hybrid centrality measures for binary and weighted networks. In: Complex Networks. Springer: Berlin. 2013;424.

[118] Koschützki D, Schreiber F. Centrality analysis methods for biological networks and their application to gene regulatory networks. Gene Regul Syst Bio. 2008;2:193–201.

[119] Alsner J, Andreassen CN, Overgaard J. Genetic markers for prediction of normal tissue toxicity after radiotherapy. Seminars in Radiation Oncology. 2008;18:126–135.

[120] Andreassen CN. Can risk of radiotherapy-induced normal tissue complications be predicted from genetic profiles? Acta Oncologica. 2005;44:801–815.

[121] Conesa A, Nueda MJ, Ferrer A, Talon M. maSigPro: a method to identify significantly differential expression profiles in time-course microarray experiments. Bioinformatics. 2006;22(9):1096–1102.

[122] Schliep A, Steinhoff C, Schönhuth A. Robust inference of groups in gene expression time-courses using mixtures of HMMs. Bioinformatics. 2004;20:i283–i289.

[123] Magni P, Ferrazzi F, Sacchi L, Bellazzi R. TimeClust: a clustering tool for gene expression time series. Bioinformatics. 2008;24(3):430–432.

[124] Sivriver J, Habib N, Friedman N. An integrative clustering and modeling algorithm

for dynamical gene expression data. Bioinformatics. 2011;27(13):i392–i400.

[125] Michna A. splineTimeR: Time-course differential gene expression data analysis using spline regression models followed by gene association network reconstruction. R package version 100. 2015;.

[126] Aryee MJ, Gutiérrez-Pabello JA, Kramnik I, Maiti T, Quackenbush J. An improved empirical bayes approach to estimating differential gene expression in microarray time-course data: BETR (Bayesian Estimation of Temporal Regulation). BMC Bioinformatics. 2009;10(409).

[127] Acosta JC, O'Loghlen A, Banito A, Guijarro MV, Augert A, Raguz S, et al. Chemokine signaling via the CXCR2 receptor reinforces senescence. Cell. 2008;133(6):1006–1018.

Acknowledgements

Firstly, I would like to express my sincere gratitude to my advisors Horst Zitzelsberger and Kristian Unger for giving me the opportunity to peruse my PhD at the Research Unit Radiation Cytogenetics. I appreciate all their contributions of time, ideas and founding to make my PhD experience productive and stimulating.

Secondly, I would like to thank my teammates Herbert Braselmann and Martin Selmansberger for the methodological support, inspiring - not only scientific discussions and all the fun we have had in the last few years.

I am indebted to the rest of my colleagues Marion Böttner, Randolph Caldwell, Laura Dajka, Giesela Dettweiler, Sonia Ehrt, Igor Gimenez-Aznar, Julia Hess, Steffen Heuer, Ludwig Hieber, Claire Innerlohinger, Elke Konhäuser, Sebastian Kuger, Valentina Leone, Doris Mittermaier, Daniel Phielmaier, Adriana Pitea, Ludmilla Schneider, Aaron Selmeier, Christina Wilke, Roland Wunderlich, Isabella Zagorski and Verena Zangen for any kind of support I have received during my PhD time.

A special thanks to all those who helped to realize my work, be it with technical assistance, discussions or proofreading. Without your support it would not be possible to conduct this research.

I would like to acknowledge all my project collaborators, especially Anne Dietz, Maria Gomolka and Sabine Hornhardt from the Federal Office for Radiation Protection as well as Ulrike Schötz and Kirsten Lauber from the Department of Radiotherapy and Radiation Oncology of the Ludwig-Maximilians-University in Munich for providing me with biological materials and for their valuable contributions.

Last but not the least, I would like to thank my parents Henryka and Henryk, brother Szymon and my friend Tomasz Witkowski for supporting me spiritually throughout my PhD and my life in general.